ERA23FA174 Tamarack Aerospace Party Submission

Cessna 525B Structural Departure Near KTPA

Document Number:

N/A

Revision:

IR

Date:

15 June 2024

LOG OF REVISIONS

Rev	Description	Date	Approval
00	Initial Release	15 June 2024	H. Gates

TABLE OF CONTENTS

LIST OF FIGURES

REFERENCES

[1] Office of Aviation Safety, *ERA23FA174 Systems Group Chair's Factual Report,* Washington, DC: National Transportation Safety Board, 2024.

[2] Office of Research and Engineering, *ERA23FA174 Materials Laboratory Factual Report 23-051,* Washington, DC: National Transportation Safety Board, 2024.

[3] Office of Research and Engineering, *ERA23FA174 Airplane Performance Study,* Washington, DC: National Transportation Safety Board, 2024.

[4] P. L'Allier and N. Olson, *TAG-1103-0029 Wing Loads,* Tamarack Aerospace Group, 2017.

[5] N. Olson and K. Woodruff, *TAG-1103-0030 Flight Test Validation of Loads,* Tamarack Aerospace Group, 2017.

[6] B. Stevens, *TAG-1103-0049 525B Winglet Static Test Plan,* Tamarack Aerospace Group, 2017.

[7] B. Stevens, *TAG-1103-0051 Winglet Static Test Report - 525B,* Tamarack Aerospace Group, 2017.

***Tamarack Aerospace Group certification reports contain proprietary design data outside of information referenced in this document and are not intended for public distribution**

1 INTRODUCTION

On March 30, 2023 at approximately 1815 EDT (2215 Zulu), a Cessna 525B was involved in an accident during a descent through approximately FL300 over the Gulf of Mexico at approximately 275 KCAS. The accident flight was planned from Walnut Ridge, AR (KARG) to Fort Myers, FL (KFMY). The accident airplane was equipped with Tamarack's active winglet installation (wing extensions, winglets, and the proprietary load alleviation system called ATLAS). The pilot reported experiencing "two big jolts," in the form of two sequences of negative G, followed immediately by positive G, within approximately a second. After these "jolts," the pilot observed that the left hand winglet had departed the airplane, while the right hand winglet was still attached. The pilot declared an emergency, diverted to Tampa (KTPA), and made an emergency landing. The pilot reported some binding of the ailerons on final approach to Tampa, but reported no major flight anomalies and was able to complete the landing safely. The pilot was the sole occupant of the airplane and was uninjured.

1.1 Submission Abstract

- Tamarack was initially contacted by the operator of the airplane to report the incident. The NTSB opened an investigation shortly after, and asked Tamarack to join on the basis of expertise in the damaged structure. Tamarack personnel traveled to Tampa to examine the accident airplane.
- The left hand wing extension was mostly departed from the airplane, except for a small portion of the inboard structure near the joint to the OEM structure and a significantly damaged portion of the leading edge. The wing extension structure outboard of the remnant structure was not recovered, nor was the left hand TACS.
- The winglet was not initially recovered, but was found by a private boat in the Gulf of Mexico 11 days after the accident and turned over to the NTSB.
- All ATLAS components were tested, using ATLAS' built-in test with the components still installed in the airplane during initial examination and via the manufacturer's approved Acceptance Test Procedure at the manufacturer's facility after removal from the airplane. All components were found to be functioning properly and passed ATP.
- A red mark on the winglet tip, a color not present in the aircraft livery, indicates contact between the winglet and an unknown foreign object.
- Fastener failure mode examinations, supported by finite element analysis of possible abnormal load scenarios, indicate that the most likely accident sequence involves a structural failure starting from the forward edge of the upper wing extension forward spar
- Tamarack concludes that the airplane suffered a collision with an unknown object on the ground which reduced the structural margins of the wing extension, enabling a chain reaction of structural failures that led to the departure of the wing extension and winglet in flight.

1.2 ATLAS Overview

Tamarack Aerospace Group manufactures a modification for Cessna 525 airplanes, consisting of aluminum wing extensions, composite winglets, and a proprietary load alleviation system known as the Active Technology Load Alleviation System (ATLAS). ATLAS is an analog electromechanical system designed to measure vertical accelerations on the airplane and automatically deploy aerodynamic surfaces to counteract structural loads. The system consists of an ATLAS Control Unit (ACU) mounted near the center of the airplane, which provides command signals which deploy Tamarack Active Camber Surfaces (TACS) at the wingtip via extensions or retractions of linear actuators mounted in TACS Control Units (TCUs). The TCUs are linked to the TACS by conventional linkages. In the event of a fault, the ACU sends a signal to an Annunciator LRU, which illuminates LEDs within an ATLAS INOP Button located in the upper left portion of the pilot's side of the instrument panel. The button functions both as the primary indication of ATLAS fault conditions, and the primary means by which the pilot can reset faults. A view of the four main LRUs involved in the installation is presented in Figure 1-1.

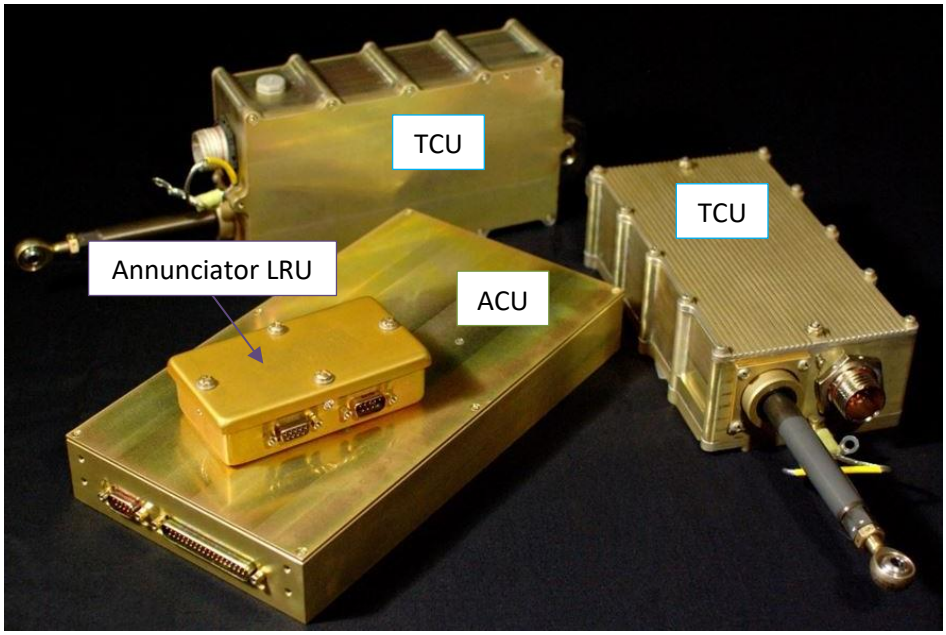

Figure 1-1 ATLAS LRU overview

An overview of the locations of LRUs in the airplane installation is presented in Figure 1-2.

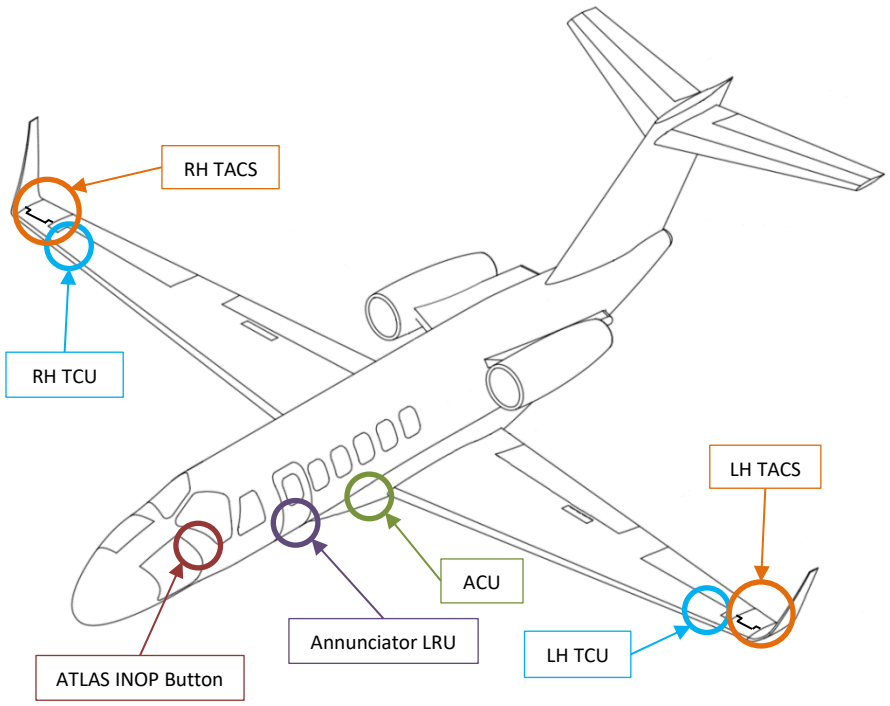

Figure 1-2 LRU locations in representative 525-series installation

For additional reference, a cutaway image of the wing extension and TACS deployment linkages is provided in Figure 1-3.

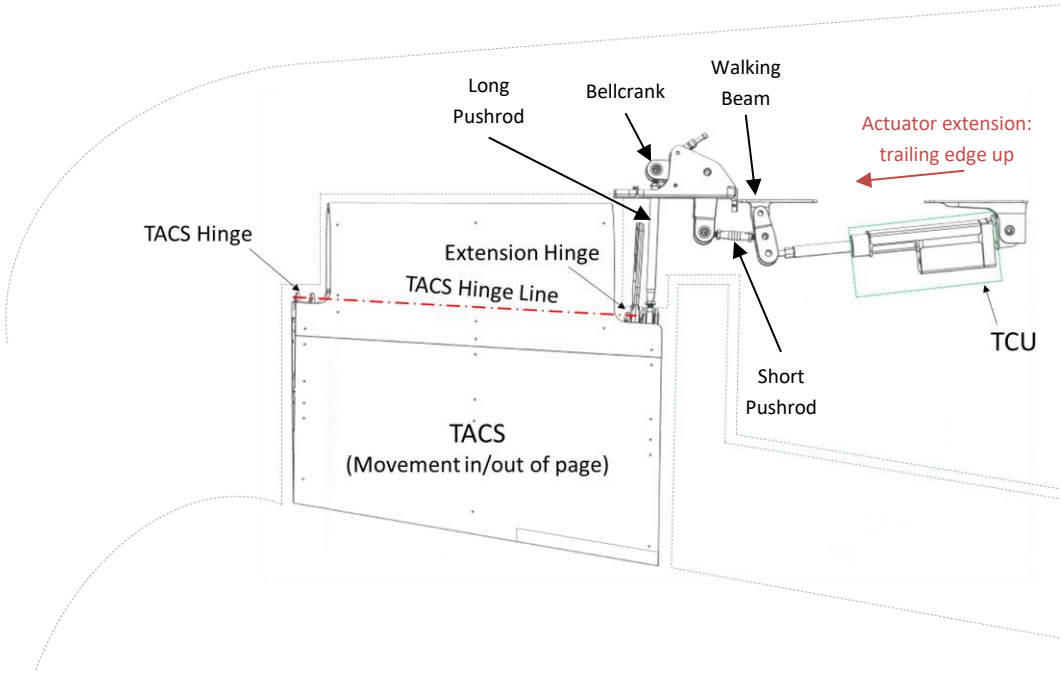

Figure 1-3 TACS deployment linkages detail

2 OVERVIEW OF INVESTIGATION

2.1 ATLAS Equipment

During the initial examination of the airplane in a hangar at Tampa, the party specifically examined the ATLAS electronic LRUs, as well as the remaining components related to moving the TACS. The right hand side of the airplane was found intact, with all components correctly installed and properly secured. The left hand side of the airplane sustained significant damage, including damage to long pushrod between the bell crank and the TACS. The bell crank on the left side exhibited small marks indicating light contact between the faces of the bell crank arms and the bell crank hard stops. These marks are not uncommon in ATLAS installations, and are consistent with light contact during installation and ongoing preflight inspections, when personnel on the ground move the TACS by hand and the bell crank to touch the hard stops.

The long pushrod on the left side was found fractured near threads at the end closer to the TACS. The remains of the long pushrod was found resting on the upper surface of the aileron control horn, rubbing the aileron control horn as the aileron was moved. Hand movement of the aileron during initial examinations could not discern any evidence of binding internal to the aileron hinges. The contact between the broken pushrod and the aileron control horn most likely accounts for the binding reported by the pilot. The broken pushrod was removed to prevent damage to other components on the left hand side during the rest of the examination.

The aircraft battery was connected, and the ATLAS built-in test was performed to ascertain the status of the system as found. The system powered up normally, without faults. The built-in test executed normally, indicating the system was functioning properly.

The ACU and both TCUs were removed from the plane, and were sent to the NTSB for CT imaging. The CT imaging did not find any defects or failures within any of the examined units. The LRUs were then sent for lab testing at the manufacturer's facility in Wichita, KS. Each LRU passed the approved Acceptance Test Procedure (ATP).

Therefore, these tests conclude that ATLAS was in a functional state during the accident event.

2.2 525B Flight Envelope and Flight Test Comparison

A performance evaluation conducted by the NTSB found that the airplane was descending at approximately 5,300 feet per minute at the point of separation, between approximately 29,000 feet and 30,000 feet above sea level (between FL290 and FL300). The descent rate appeared to be related to altitude requirements at intersection OGGER, which is part of the TYNEE TWO arrival procedure for Fort Myers airport. The airspeed during the descent appeared to be close to VMO/MMO throughout, peaking

at approximately 276 KCAS at the estimated point of departure of the LH wing extension and winglet. A trace of the airplane's airspeed at various altitudes is presented below. Note that the accident flight is in red. Other traces are visible in the figure below, corresponding to flight test data collected by Tamarack during the certification flight test program for ATLAS installations on the 525B.

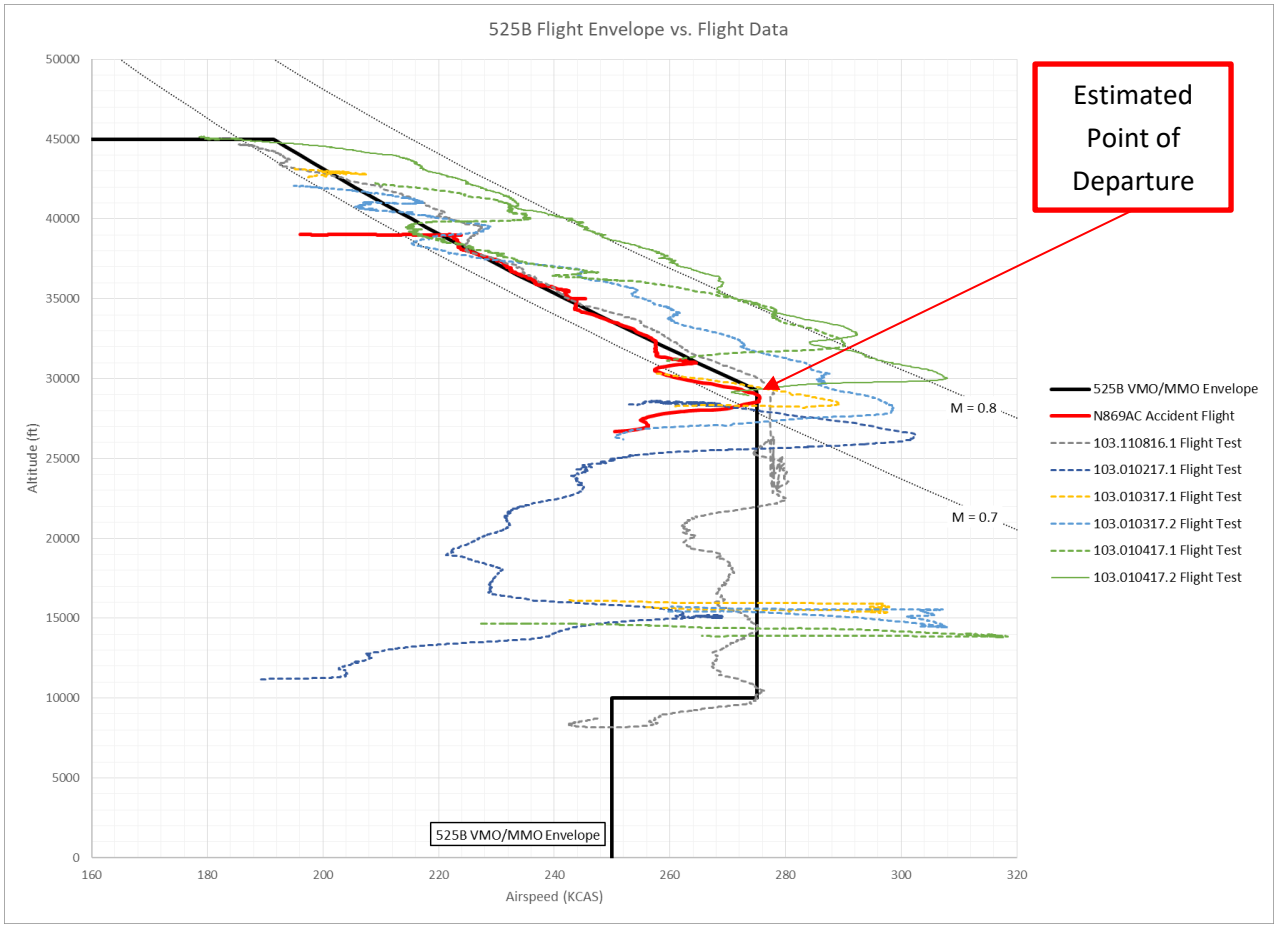

Figure 2-1 Accident flight and flight test comparison to flight envelope

Tamarack notes that at approximately FL300, the flight envelope transitions from VMO (speed) to MMO (Mach number) as the speed limit for the airframe. This point is called the "knee" altitude, and represents the highest simultaneous Mach and dynamic pressure that the airframe can experience in flight. A detail view is presented below, showing the same flight data but scaled to focus on the knee region.

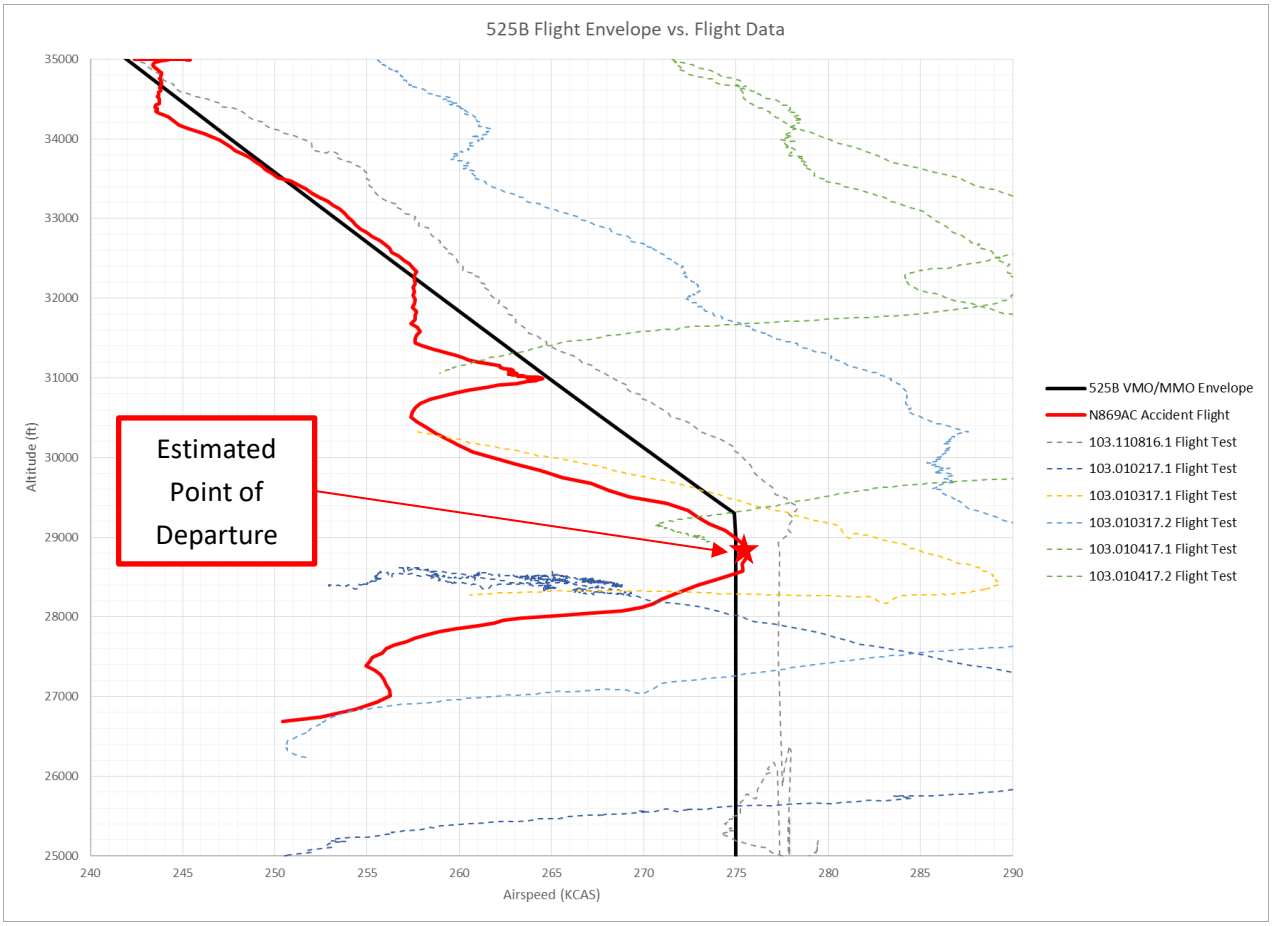

Figure 2-2 Accident flight and flight test comparison, detail at envelope knee

In the figure above, the accident flight is represented by a solid red line, while Tamarack flight test data is represented by dashed lines of different colors. Tamarack notes that VMO for the 525B is 275 KCAS, and the accident flight appears to have peaked at 276 KCAS. Tamarack also notes that certification authorities required flight testing at speeds well in excess of the VMO/MMO envelope as part of the approved flutter flight test program. Furthermore, structural analysis of the 525B ATLAS installation developed aerodynamic loads based in part on speeds above VMO/MMO at the knee altitude, ensuring that the analysis fully envelopes the most severe conditions encountered in service. While these high speeds are explicitly not permissible for flights in normal operation, the flight test data demonstrates that the airplane has been thoroughly tested in conditions more severe than the accident flight and that the flight condition alone was not a contributing factor in the separation of wing extension and winglet structure.

2.3 525B Structural Loads and Testing Comparison

Structural loads were developed for the 525B during ATLAS certification in an EASA-approved and FAA-validated loads report. This report considered thousands of loads cases to determine the most critical loads on the airplane structure. A selection of load cases is presented in APPENDIX A of this document. The load cases and model developed in the loads report were then validated with flight test data, reported in a similarly approved flight test validation report.

The flight test validation report recalculated critical loads using the validated model and added loads cases with speedbrakes to determine the final loads envelopes. Note that these loads cases cover the entire airspeed envelope up to V_D (the aircraft dive speed, a certification requirement above the VMO/MMO limit), the entire CG envelope, and all required maneuvers and gusts for all required configurations of the aircraft (clean, flaps, ailerons, speedbrakes, ATLAS failures, etc.). All loads presented in the loads reports are limit loads; the maximum intensity loads that the airplane will encounter in service.

Examining the wing extension and winglet more carefully, the critical loads cases for vertical shear, bending moment and torsion consist of 3 types of loads cases, a limit gust with ATLAS operative, a limit gust case with ATLAS inoperative, and a yaw maneuver required for commuter category aircraft. Except for the ATLAS inoperative gust case, the critical cases occurred at V_D. More details of the critical winglet and wing extension cases are presented in APPENDIX B.

Structural testing of aircraft structures must include ultimate load cases, defined as 150% of limit loads, and the structure must be able to withstand those loads for at least three seconds. This requirement ensures that all aircraft structures are safe and capable of withstanding the most severe normal operating aerodynamic loads with clear margin of safety.

The wing extension, winglet and furthest outboard rib bay of the OEM wing were tested beyond ultimate loads without failure (to approximately 180% of limit load). Testing was conducted according to an EASA-approved and FAA-validated static test plan, and results were reported in detail in a similarly approved and validated static test report. The winglet and wing extension were tested separately for both up bending and down bending cases. The load application points were chosen such that critical torsion loading was also included. The net result of this test setup is that the wing extension was subjected to test load more severe than required by the certification regulations, combining multiple types of loading simultaneously, without failure.

Importantly, the final test case in the wing extension static test plan was an intentional structural failure case. Following successful limit, ultimate, and higher-than-ultimate tests, load was applied to the wing extension until failure occurred. Failure testing is commonly conducted to establish the actual margin of safety of a structure and to help validate analytical models. In this case, the failure did not occur in the

wing extension, but rather several inches inboard of the inboard edge of the wing extension, in the OEM section that had been constructed for testing.

Applicable regulations for the winglet test were EASA CS-23/US 14CFR 23.303, 23.305, 23.307(a), 23.613(c), and 23.641. The carbon fiber winglet had Barely Visible Impact Damage (BVID) conservatively applied prior to the limit load test by dropping a steel rod from just over 37 inches to achieve a required 25 ft-lb of impact energy. BVID testing is required for composite structures to simulate damage and defects within the carbon fiber structure. Note that BVID is not required for conventional aluminum structures. Each winglet test article had the BVID procedure completed for 10 target locations on the composite structure. After the BVID was applied, the test articles underwent tests at 100%, 120%, 150%, and 180% of limit load, followed by an intentional failure test for both up and down bending.

During the up-bending test, the winglet held 1,860 lbf for more than 3 seconds before failure. Limit load was 797 lbf, meaning failure occurred at 233% limit load. During the down bending test, the winglet held 1,721 lbf for more than 3 seconds before failure. Limit load was 790 lbf, meaning failure occurred at 218% of limit load. The TACS were tested to 171% of limit load without failure. The wing extension underwent 3 tests to cover the loads envelope.

A down bending test and two up bending tests, one to cover the upward bending moment and one for the upward vertical shear, were conducted. The vertical shear test was the more critical of the two. Each of the three tests were tested to 100%, 150%, and 180% of limit load with the upward shear test being tested to failure at 4280 lb. Limit load was 1695 meaning failure occurred at 252% of limit load.

The static testing completed on the winglet, TACS, and wing extension prove that the ATLAS-associated structure is designed and built stronger than required by flight loads, with a significant margin of safety. Thus, it is not possible that normal flight loads in general and the accident flight condition at the time of structural separation in particular could have caused the overstress conditions apparent in the wreckage alone.

3 DETAILED ANALYSIS

3.1 Specific Areas of Focus

Several areas of the recovered structure were of particular interest during the investigation:

1. A flattened area at the outboard portion of the leading edge of the LH wing extension.
2. A red mark on the LH winglet tip cap, which does not match any color on the rest of the airplane.
3. Forward spar fastener failures, specifically near the forward section of the upper forward spar.

3.2 Leading Edge Flattening

An initial theory of the cause of the accident involved a possible impact with a foreign object mid-flight. The key piece of evidence that initially supported this theory was the condition of the wing extension leading edge, which featured a flattened section, marks on the interior of the leading edge, very closely matching the shape of the winglet attachment rib in that section, and paint transfer from the rib to the interior of the leading edge. The damage initially presented as evidence of an impact with an object at the winglet attachment, which could have caused damage to the rest of the wing extension and led to failure.

A thorough investigation of the remaining wing extension structure and the winglet upon recovery did not turn up further supporting evidence of this theory beyond inconclusive faint scratch marks on the leading edge. There was no evidence of organic material or residue on any surface of the wing extension tested by blacklight, indicating that the airplane did not strike a bird. The leading edge wing extension and winglet did not exhibit the type of damage typical of impact with a drone or other solid object in flight. Review of radar data and amateur radiosonde balloon tracking applications did not show any high-altitude balloons in the area at the time of the accident.

To explain the presence of the flattened leading edge section and interior marks a simple company test was designed and conducted using a scrap wing extension forward spar assembly, scrap winglet closeout rib, and scrap leading edge. The test was designed to simulate the winglet rib nose twisting out of the leading edge to determine potential causes for the leading edge flattening and internal marks found on the accident airplane.

The test setup was a simple wooden fixture base with a scrap extension forward spar and leading edge assembly fixed to it. A winglet attachment rib was installed as it would be in an airplane installation, with a riveted angle bracket and two screws in the leading edge. The rest of the leading edge screws were installed in the forward spar caps as they would be in the airplane. A steel lever arm was fabricated and bolted into existing fastener holes in the winglet attachment rib, providing a place to apply a moment on the assembly. An image of the test setup is presented below.

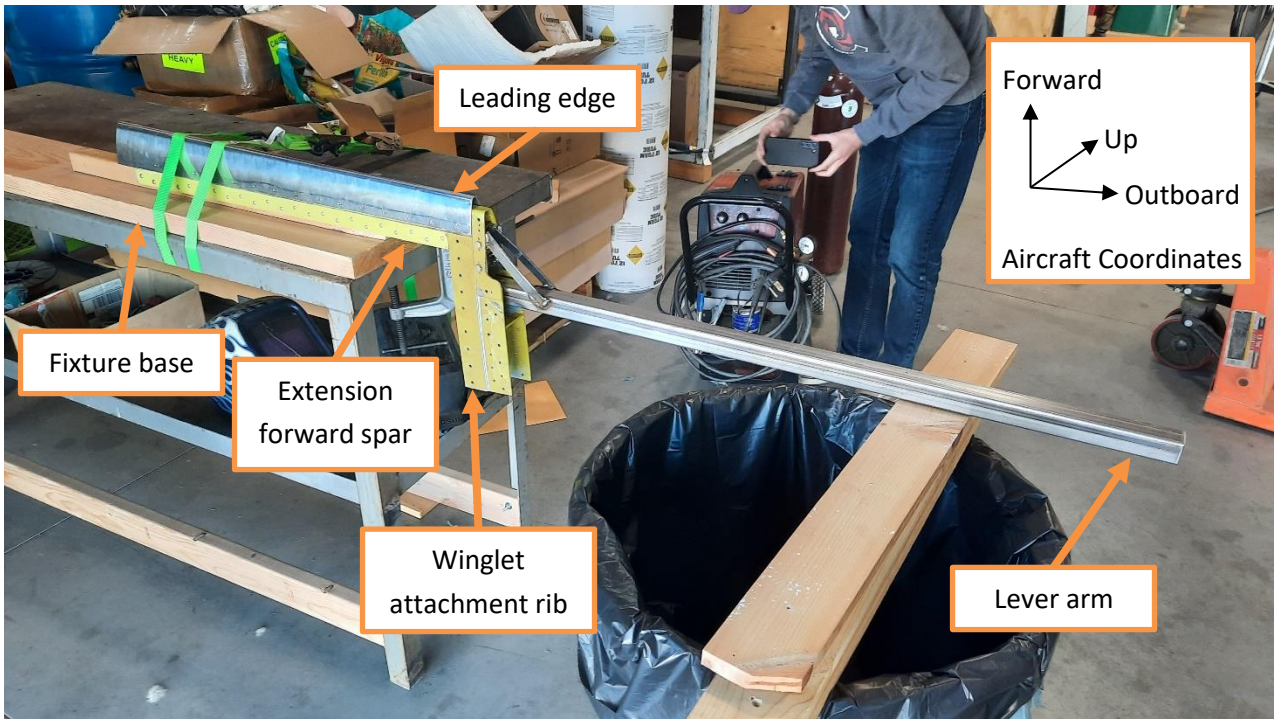

Figure 3-1 Company winglet rib tear-out test setup

The wing extension skin was removed for this test, to simulate the wing extension assembly after the loss of the upper and lower skin during the accident event and to allow the winglet attachment rib to rotate around the forward spar easily during the test.

The test article was oriented with the leading edge pointing up, so that a simple downward hand load could be applied to the lever arm. This simulated the winglet twisting outboard about its vertical axis and rotating the attachment rib out of the leading edge around the end of the forward spar.

During the test, the winglet attachment rib separated from the forward spar assembly by fracturing the angle bracket riveted to the rib and tearing the two attachment screws out of the leading edge fastener holes. Some of the damage noted during the test resembled damage observed on the airplane, particularly drag marks within the leading edge, deformation of the leading edge skin, and fracturing of the rib attachment angle bracket.

A series of images is presented below to compare aircraft damage to test damage.

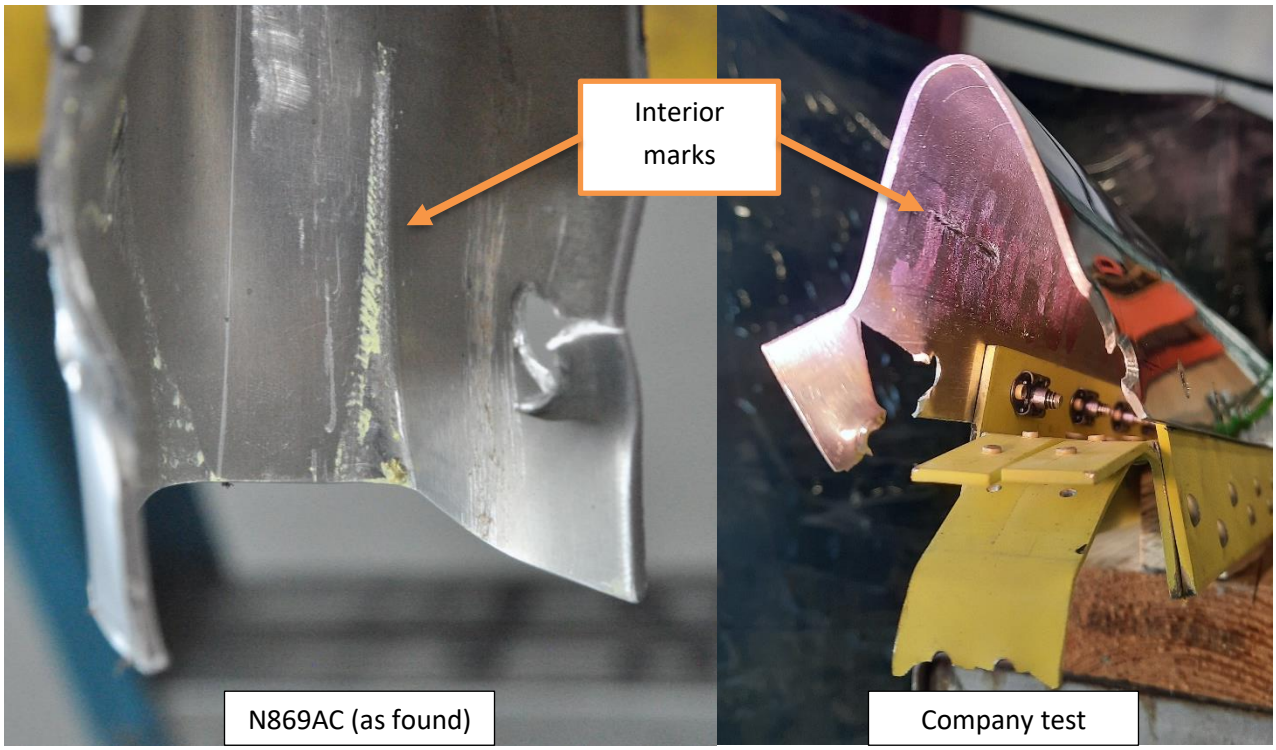

Figure 3-2 Aircraft damage vs. test damage - leading edge interior marks

During the company test, the forward edge of the rib dragging along the interior of the leading edge skin caused deformations similar to those found on the accident airplane. Notably, the company test was less dynamic and destructive than the accident sequence appears to have been, and the deformation is therefore less pronounced than the flattening of the leading edge discovered on the accident airplane. However, the company test article deformation is of a similar type and in a similar location. A reflection of

graph paper is used to demonstrate the location of deformation of the company test article leading edge in the following comparison image.

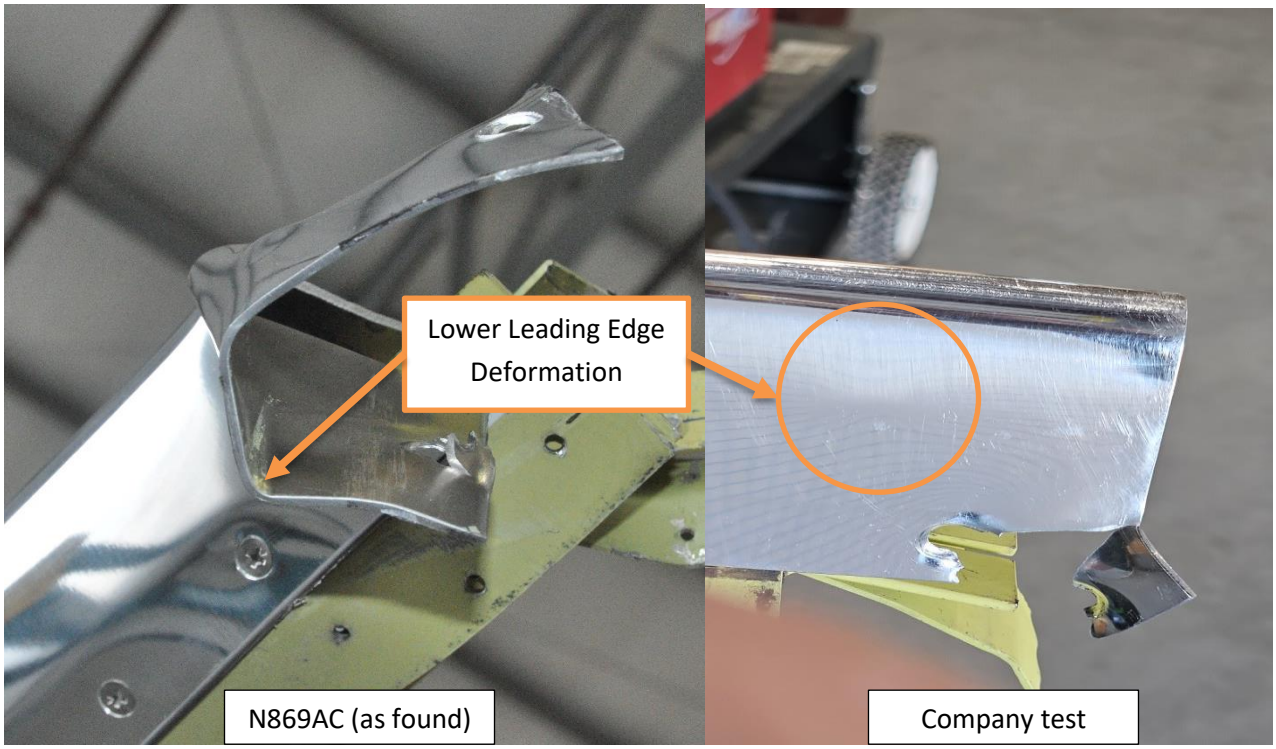

Figure 3-3 Aircraft damage vs. test damage - leading edge deformation

Tearing of the leading edge skin around the fasteners in the winglet attachment rib was similar in both the accident airplane and the company test article following the test, as shown below.

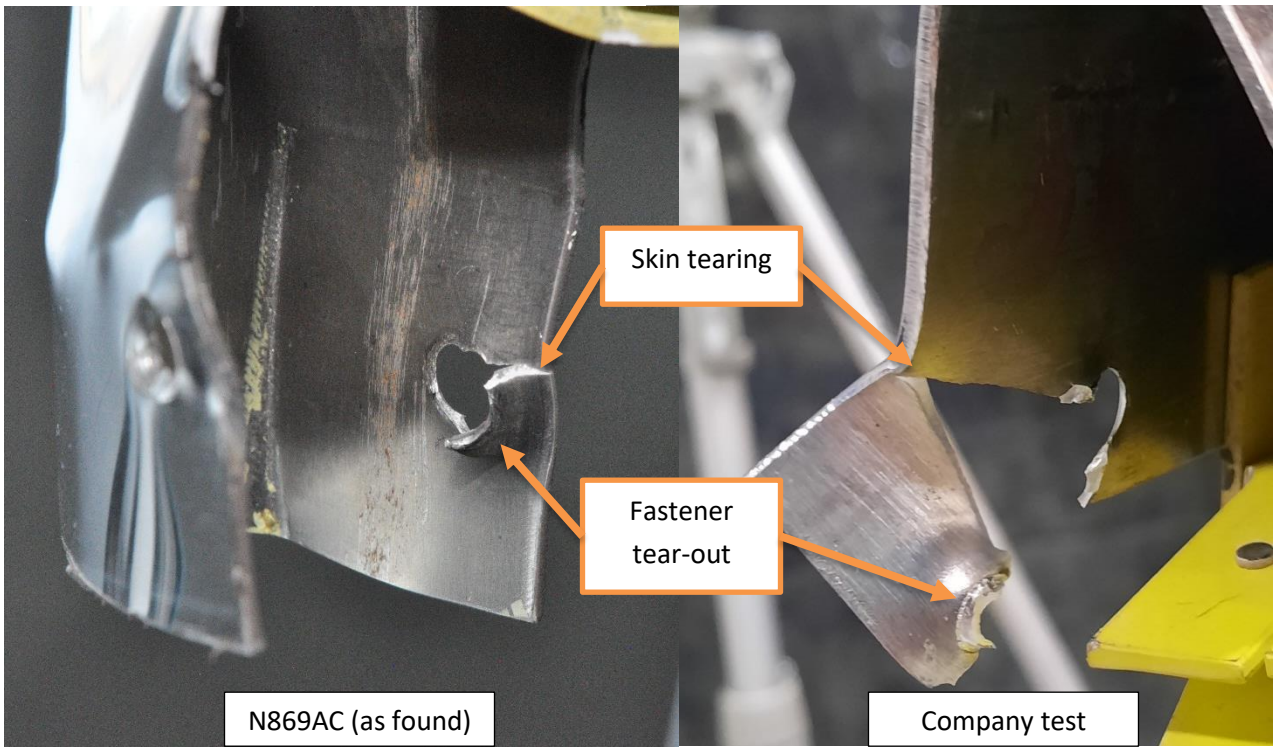

Figure 3-4 Aircraft damage vs. test damage – fastener damage and skin tearing

While the company test conditions were different than the more rapid onset, more dynamic, multi-axis loading most likely experienced by the accident airplane, the key similarities between the company test article and the accident airplane damage lead Tamarack to conclude that it is possible to create the flattened section and marks on the interior of the leading edge without an external impact.

3.3 Winglet Tip Cap Mark

The winglet was recovered by a fishing boat shortly after the initial inspection of the airplane was conducted in Tampa, and was found with a red mark on the winglet tip cap. The red mark is of particular interest, because the airplane paint scheme does not include red, the primer used on the winglet is not red, and the structure of the winglet itself is not made of any red material. The red mark therefore could only have been caused by contact with some other object.

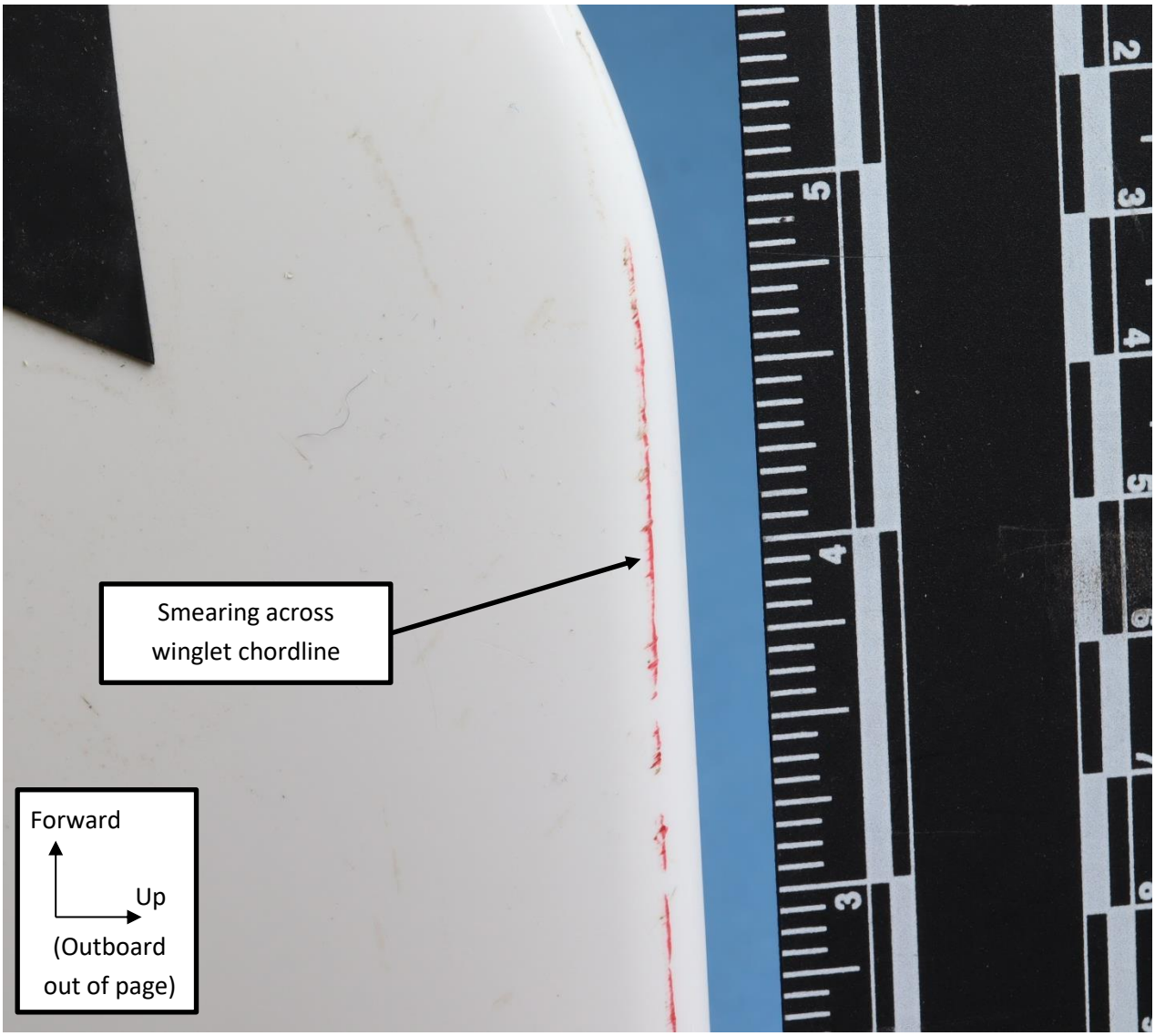

Figure 3-5 Winglet tip cap red mark

It is improbable that this contact occurred in flight, specifically that the airplane would have passed close enough to another aircraft or UAS at that altitude for the winglet to make contact and transfer paint without the other aircraft or UAS being visible either to radar or the pilot. It is also improbable that contact would be limited solely to a single red paint transfer on the winglet tip and not involve any other obvious damage to the structure of the winglet, especially considering the speeds involved during the accident event.

Testing conducted at the NTSB materials lab concluded that the red mark chemical composition was consistent with automotive and industrial paints in common use and was similar to the aircraft topcoat. That color is not used anywhere on the airplane, and therefore must have transferred from a different object. The shape of the marks indicates dragging or scratching across the chordline of the winglet.

A mark of this type is improbable in flight, but can occur during hangar rash and ground handling mishaps. Tamarack customer service personnel have responded to at least ten reported incidents of ground contact with other airplanes, hangars, and vehicles since ATLAS certification. Of the reported incidents, seven have involved varying degrees of confirmed structural damage. An example of damage on a different airplane involved in a confirmed ground collision is presented below for reference.

Figure 3-6 Example of confirmed ground damage (separate incident)

Note that the damage shown above is clearly visible on a standard walkaround inspection. The leading edge of the winglet collided directly and forcefully with a parked airplane, causing obvious structural damage. Also note that the damage caused failures of the wing extension forward spar fasteners and deformation of the leading edge skin around the area of the winglet attachment rib, similar to failure modes observed on the accident airplane, though more obvious and severe.

The red mark on the accident airplane is located on the curve of the winglet tip cap, a location on the winglet that nominally sits approximately eight feet above ground level. This area is difficult for pilots to inspect during preflight . An image of an exemplar aircraft and exemplar pilot is presented below to illustrate.

Figure 3-7 Winglet tip height reference image

Even for a taller pilot, the area at the winglet tip is difficult to see during preflight inspections, particularly the area in the curve of the winglet tip cap where potential marks would be above eye level and partially obscured.

It is possible that a glancing impact with an object during ground handling of N869AC prior to the accident flight caused a load exceedance in the structure that did not produce obviously visible failures in the structure. The evidence of the impact, the red mark on the winglet tip cap, would be in an area that is not readily accessible to pilots during walkaround. The airplane in question is operated normally by multiple pilots and handled on the ground by multiple personnel. It is possible that a ground handling crew experienced the impact during ground operations. It is also possible that task saturation, the brief and glancing nature of the impact, and/or noise and vibration of a moving vehicle or machinery could have masked a glancing impact. If the impact did not register with ground personnel, it is not unreasonable to expect that the impact would not have been reported, particularly if the only evidence was in an area that is difficult to see. The exceedance caused by such an impact may have weakened fasteners and structure, resulting in a structure that appeared to be intact on preflight inspection but had reduced structural margins to carry flight loads.

The pilot for the accident flight did not report any known contact with objects on the ground during the time that he was operating the airplane on the date of the accident and did not describe any situations in which the airplane was out of his direct control for prolonged periods. It is possible that the contact occurred prior to the particular accident pilot coming into control of the airplane, and that the damage was sufficient to reduce the structural margins of key elements of the wing extension without being detectable by visual or tactile inspection during preflight.

Tamarack notes that several general aviation airplanes, particularly light single-engine piston aircraft on amphibious floats and high-wing turboprops, have wingtips that correspond to approximately the height of the CJ3 winglet tip. It is also notable that many top-swing hangar door installations use red paint for surface protection of braces and structural elements. Tamarack acknowledges that these statements are not conclusive proof, and that it is highly improbable that a positive identification of the hypothetical object will be possible, but evaluates these statements as possibilities for the source of the red mark on the winglet tip cap.

3.4 Wing Extension Forward Spar Fastener Failures

The wing extension forward spar is attached to the upper and lower wing extension skins primarily with NAS1097 solid rivets in varying grip lengths, which are common in aviation structural assemblies. The wing extension forward spar wreckage found on the accident airplane still had a large number of rivet stems in place in the forward spar. Examination of the wing extension forward spar rivets focused on determining

the failure modes of each fastener. The materials lab report details this examination in a series of figures (see below for an example of the upper surface fasteners)

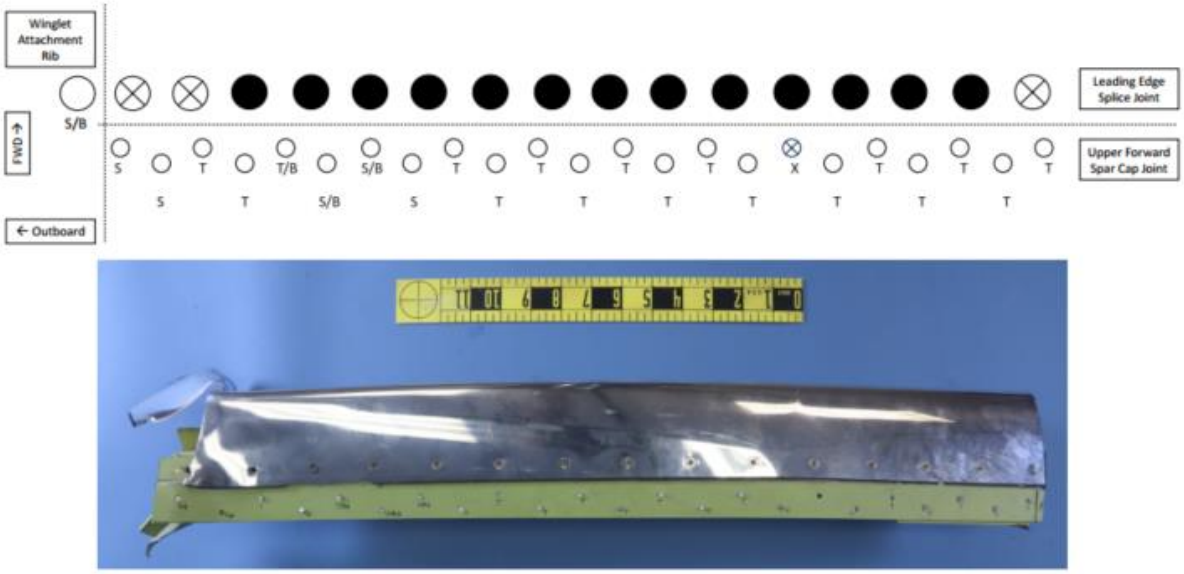

Figure 25. Schematic of the upper leading edge splice joint and upper skin-to-forward spar fastener conditions along the wing extension. Fractured fasteners are identified by an open circle, missing fasteners by a circle with an "X" and intact fasteners by a filled circle. Fracture designations are T = tensile fracture mode, S = shear fracture mode, B = mixed mode bending fracture used in conjunction with T or S as applicable.

Figure 3-8 Figure 25 from NTSB materials lab report - forward spar upper surface fasteners

The upper surface rivet failures were largely tensile, consistent with a lifting or peeling action of the upper skin of the wing extension. The outboard fasteners, particularly the most outboard pair of rivets,

presented as shear failures. The winglet attachment rib was also recovered with rivets stems, and was similarly examined, as shown below.

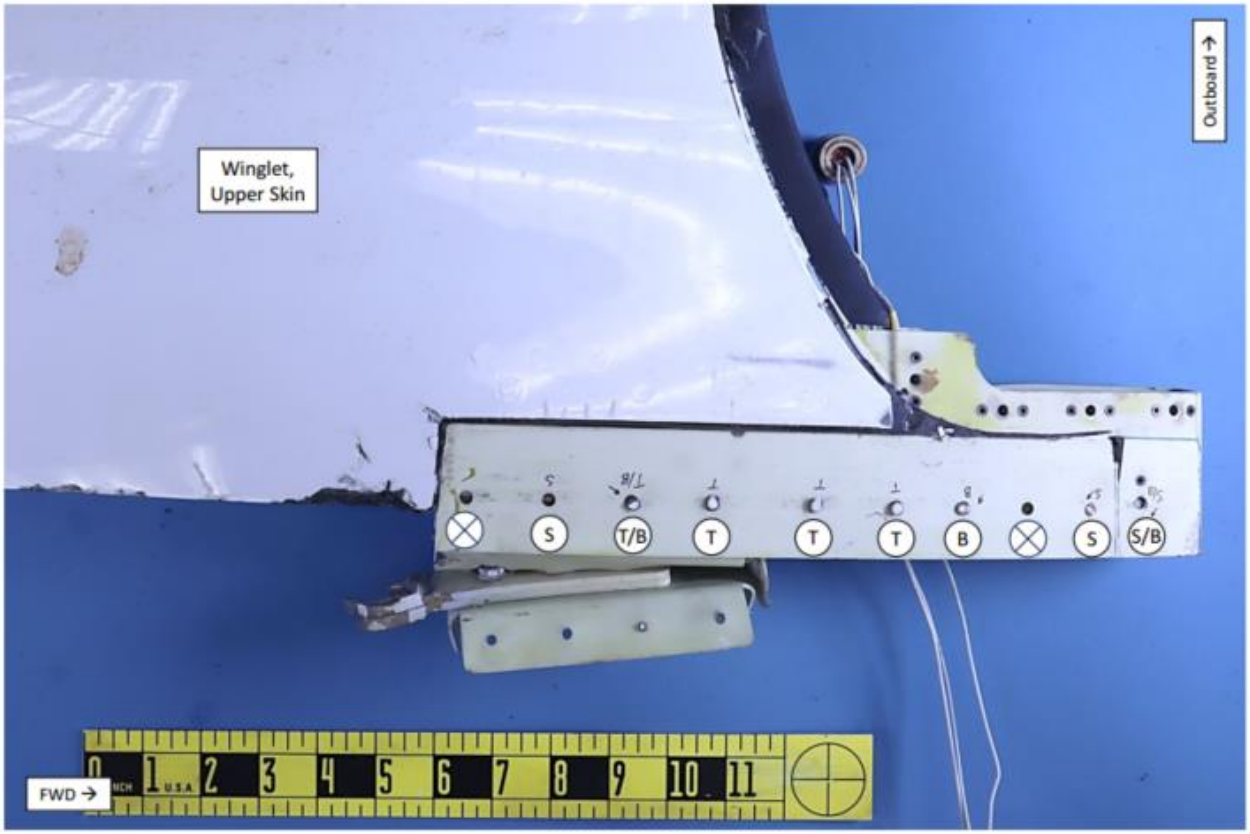

Figure 27. Schematic of the wing extension upper skin-to-winglet attachment rib fastener conditions. Fractured fasteners are identified by an open circle, missing fasteners by a circle with an "X" and intact fasteners by a filled circle. Fracture designations are T = tensile fracture mode, S = shear fracture mode, B = mixed mode bending fracture used in conjunction with T or S as applicable.

Figure 3-9 Figure 27 from NTSB materials lab report – winglet attachment rib upper surface fasteners

Note that in the figure above, three of the four forward fasteners of the winglet attachment rib were determined to be shear or bending failures. These fasteners are installed on the wing extension side, attaching the wing extension upper surface to the inboard edge of the winglet attachment rib. This indicates that a group of fasteners in proximity to each other failed in shear or shear/bending, rather than the tensile failures consistent across the rest of the wing extension forward spar.

A Finite Element Model (FEM) was analyzed to investigate the fastener reactions to a theoretical ground load applied at the tip of the CJ3 winglet. The FEM modeled the wing extension structure, including the

end rib to which the winglet attaches and the two most outboard OEM rib bays. This FEM was built during CJ3 static testing for use in the Fatigue and DT analysis certification report, where the model was validated. Because this analysis was to investigate only fasteners on the wing extension, the winglet was modeled as a single rigid element. The direction of the load applied to the model in this case reflects the direction of the "streaks" of red paint seen on the top of the winglet: a primarily inboard load with a forward load component, applied at a single point at the tip of the winglet. The winglet tip load included a 300 lbf inboard load combined with a 150 lbf forward load. An image of the finite element analysis results is presented below.

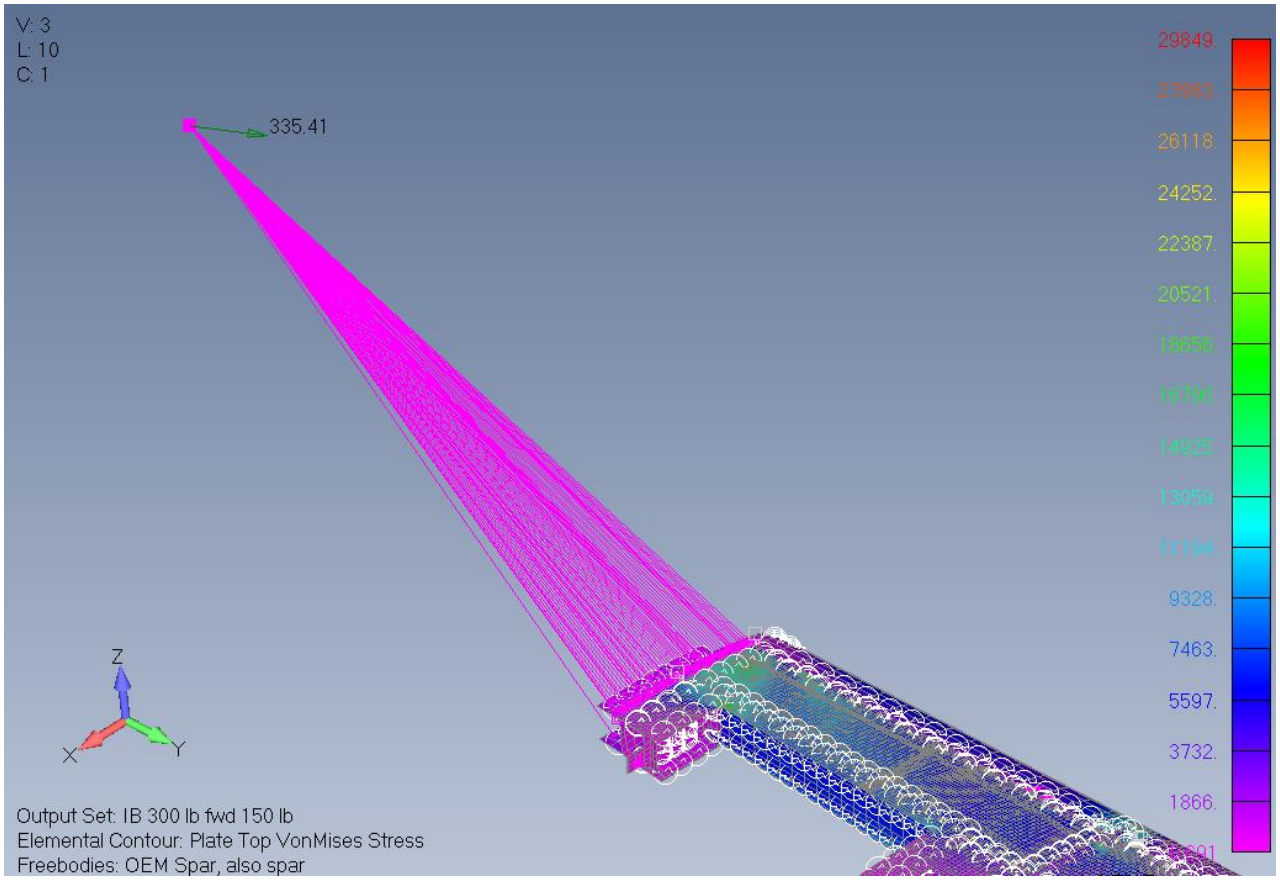

Figure 3-10 Winglet tip cap point load analysis results

Examining the fasteners common to the forward upper spar cap and upper skin revealed that they were primarily loaded in shear. The fasteners farther outboard experienced significantly higher loads than the fasteners further inboard. Under the loading conditions described above, the two farthest outboard fasteners were subject to loads higher than their prescribed shear allowable, meaning they would likely fail in shear.

Note that the load applied to the winglet tip cap in this analysis far exceeds any certification requirements, both because the magnitude of the load is larger than the realistic aerodynamic loading at this part of the structure during normal operation, and because it is applied as a single point load without any distribution. Certification requirements do not require consideration of this type of simulated ground collision load, as flight following collisions between the airplane and stationary objects is not normal operation.

Examination of confirmed ground damage incidents, and analysis of unusual, non-certification loads similar to ground collision loading, indicates that this group of fasteners tends to fail in shear when an impact between the winglet and another object occurs.

The lower surface wing extension fasteners available for examination on the forward spar showed exclusively tensile failures, as demonstrated below.

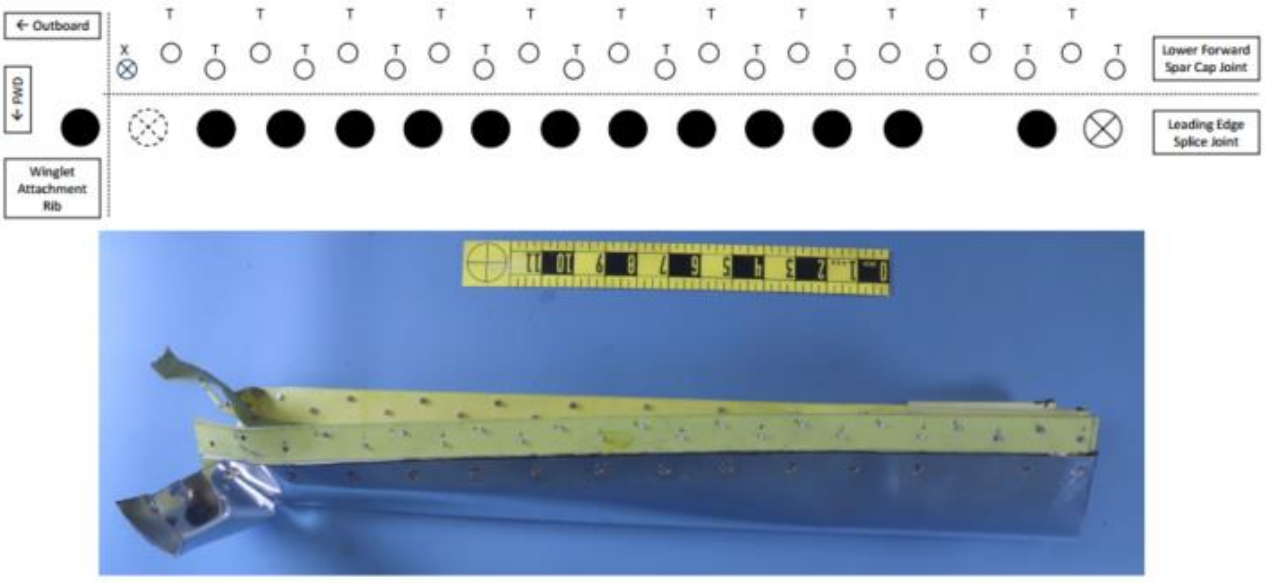

Figure 26. Schematic of the lower leading edge splice joint and lower skin-to-forward spar fastener conditions along the wing extension. Fractured fasteners are identified by an open circle, missing fasteners by a circle with an "X" and intact fasteners by a filled circle. Fracture designations are T = tensile fracture mode, S = shear fracture mode, B = mixed mode bending fracture used in conjunction with T or S as applicable. The fastener represented by a dashed "X" circle was drilled out to aid with disassembly.

Figure 3-11Figure 27 from NTSB materials lab report –extension forward spar lower fasteners

This type of failure would be consistent with a lifting or peeling of the lower wing extension skin. A small portion of the wing extension lower skin was found still attached to the lower portion of the winglet

attachment rib, deformed downward and fractured. See below for a photograph of the remaining lower skin on the winglet attachment rib.

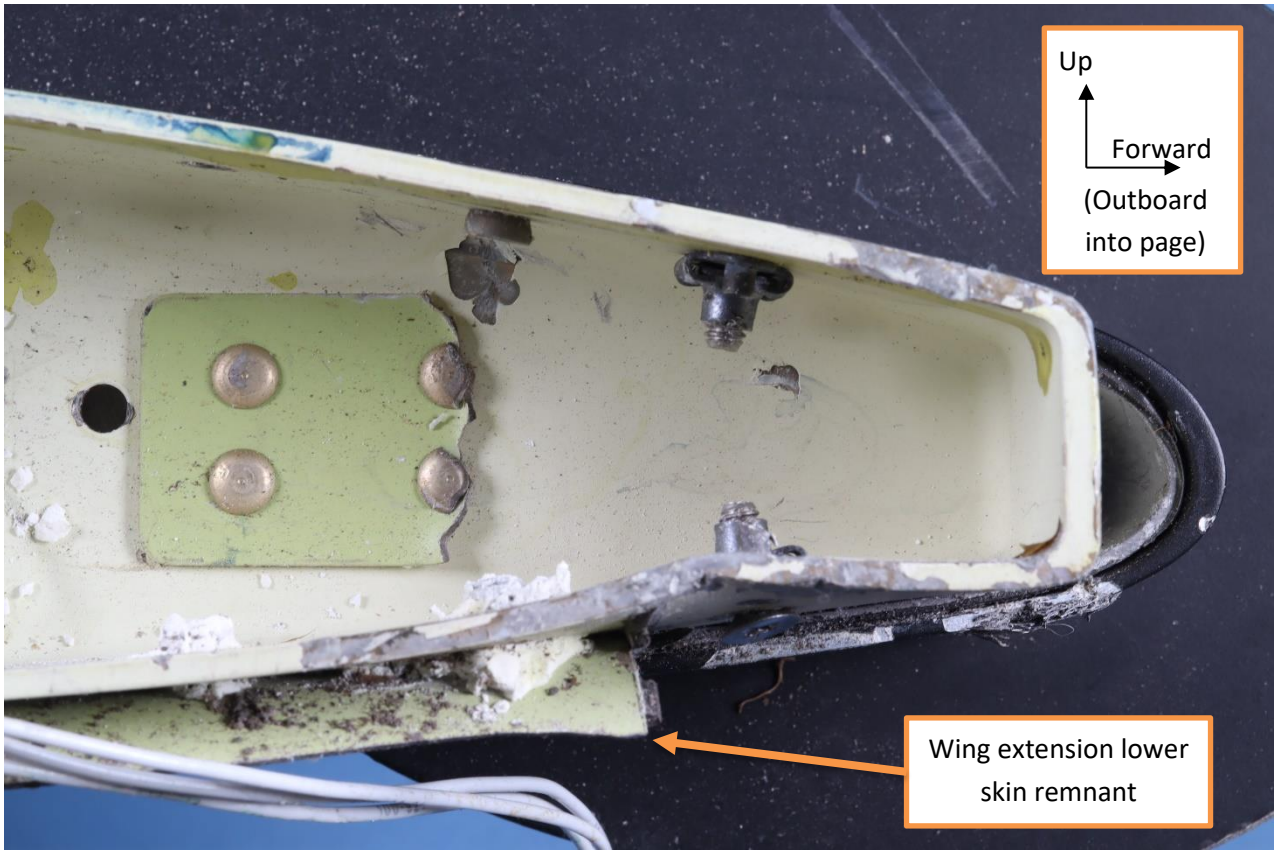

Figure 3-12 Detail view of the winglet attachment rib

The remnant lower wing extension skin is bent downward and torn, which is consistent with the winglet rotating outward around the axis of the wing extension chordline and departing the aircraft downward.

3.5 Probable Accident Sequence

Based on the evidence uncovered during the investigation, Tamarack determines that the most likely sequence of events for the separation of the wing extension and winglet is the following scenario.

3.5.1 Initial fastener failure

Evidence indicates that the forward and outboard upper surface wing extension rivets failed in shear. It is likely that these fasteners were the first failures. It is also likely that these fasteners failed during a ground incident, in such a way that they were not readily detectable to the pilot during preflight. Shear failure of a

small number of fasteners without paint disturbances above the fastener heads would not necessarily be apparent on a visual inspection.

3.5.2 Beginning of in-flight failure sequence

The failure of the outboard forward upper skin fasteners may have allowed the winglet to twist upward or bend inward and deform the upper wing extension skin, peeling the upper skin from the forward spar. It is unknown what may have caused this twisting, but normal flight operations involve a variety of changing aerodynamic loads and perturbations, particularly at higher dynamic pressures, any of which may have caused minor flexing of the structure. This could lead the upper surface to deform upward, with aerodynamic loads catching the skin and causing it to peel from the forward spar. This would cause the remaining upper surface forward spar rivets to fail in tension (consistent with fastener states observed during the investigation). A witness mark on the upper flange of the winglet attachment rib indicates contact between the winglet attachment rib and the corner of the forward spar cap, to which the leading edge is fastened, consistent with inboard rotation of the winglet and relative movement of the two components. The mark is illustrated in the figure below.

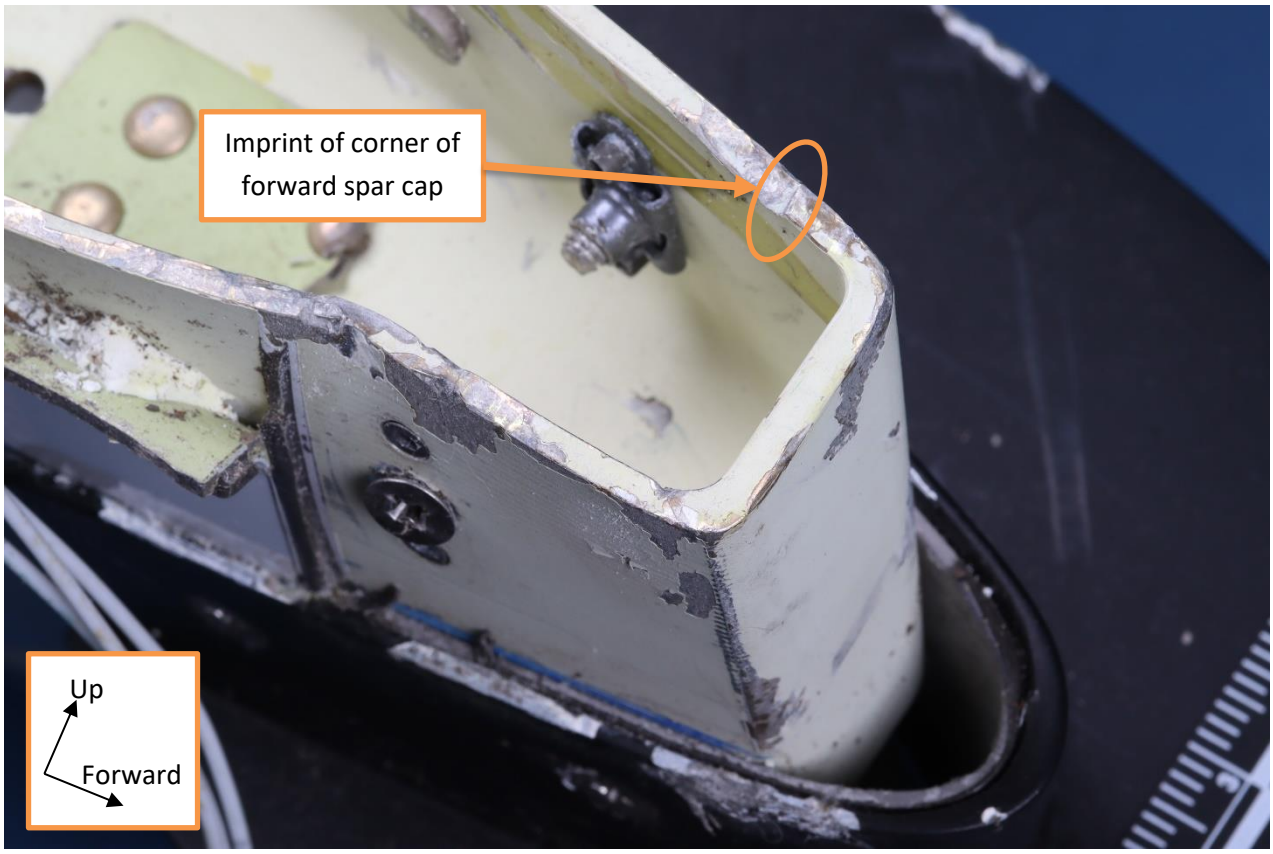

3.5.3 Departure of upper skin

If the upper wing extension skin continued to peel upward and aft, it would likely depart the airplane aft and slightly inboard. This would cause the upper flange of the outboard TACS hinge bracket to deform upward as the skin pulled it up, then cause a portion of the inboard rib upper cap at the attachment to the OEM wing to deform upward as well. This is consistent with the states of these two components as found in the investigation (see below).

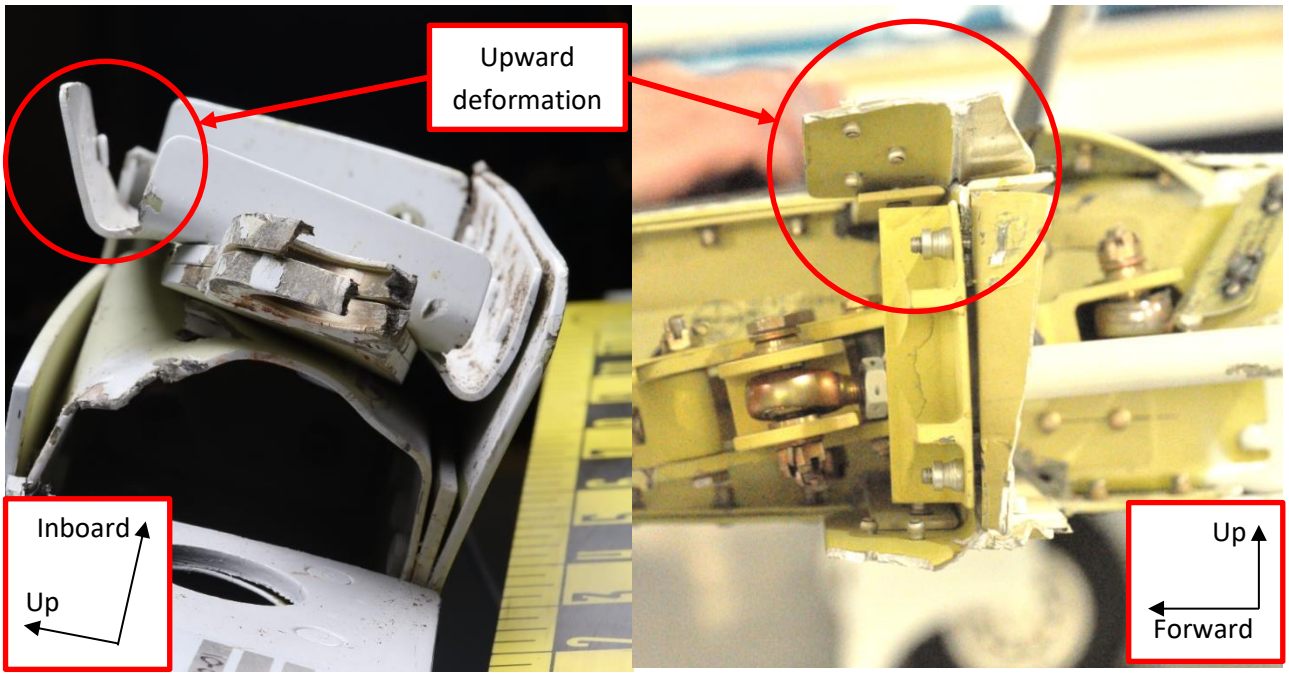

Figure 3-13 Winglet attachment rib forward view (left), wing extension main inboard view (right)

3.5.4 Winglet inboard edge damage

The departure of the upper skin would further reduce the stiffness of the winglet, allowing the winglet to twist outboard about the winglet spar and contact the TACS, causing crushing damage to the trailing edge portion of the winglet. This is consistent with damage found during the investigation, specifically in the

form of buckling of a shear clip within the aft portion of the winglet attachment rib and crushing of the carbon fiber of the aft section of the winglet itself.

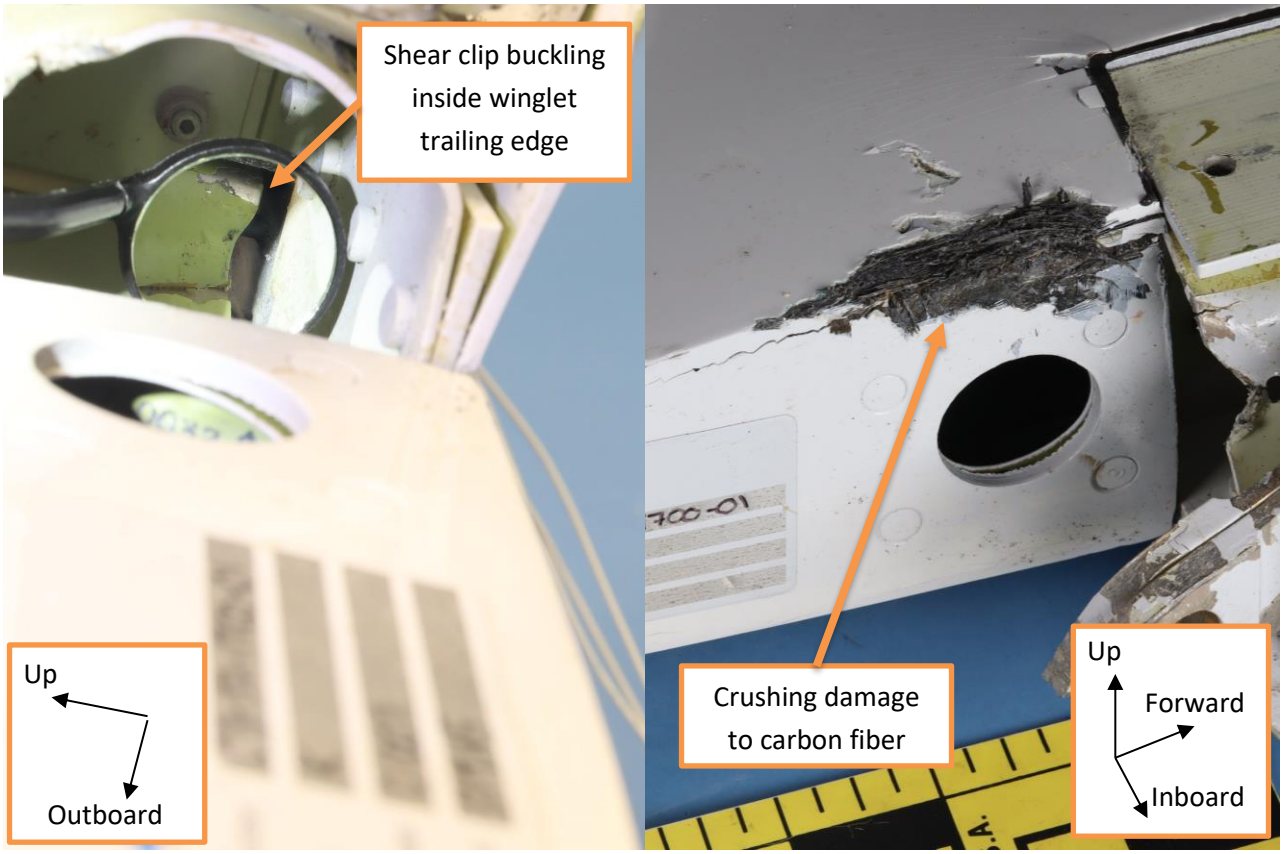

Figure 3-14 Winglet trailing edge damage due to contact with adjacent structures

The winglet could also rotate outward about the chordline of the winglet attachment rib in this state, causing buckling deformation to the winglet attachment rib at the location of the forward spar as the two components contact each other under high load.

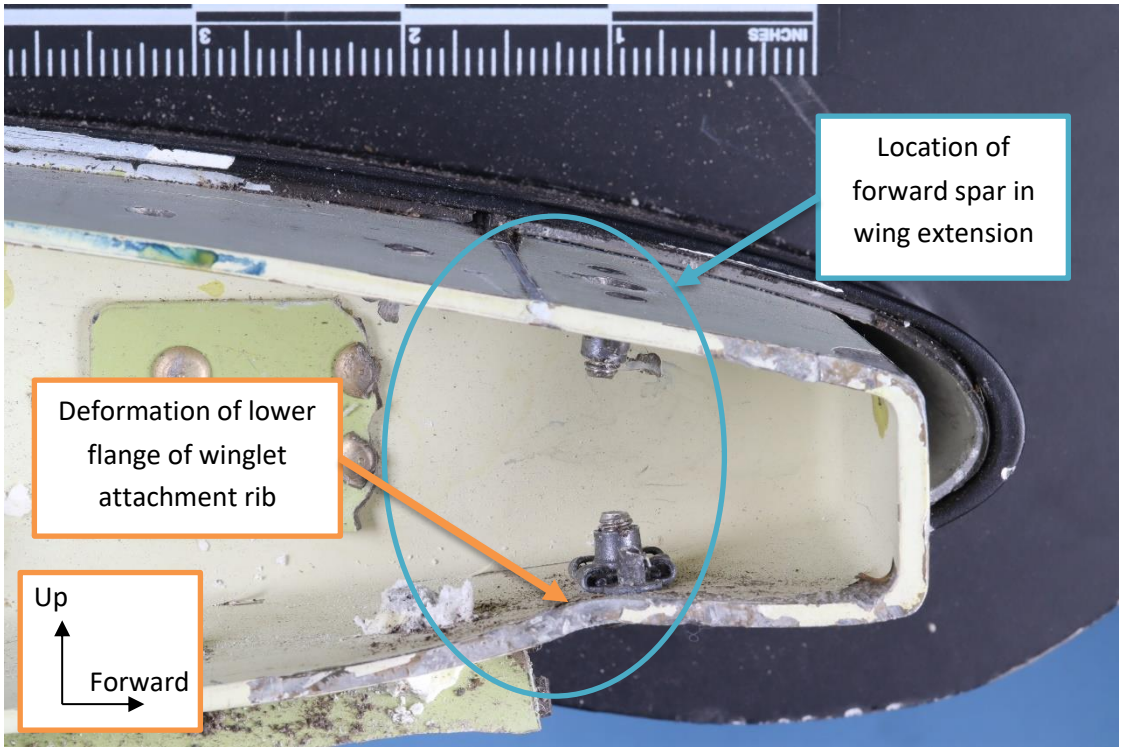

Figure 3-15 Winglet attachment rib lower flange dent (view looking outboard)

3.5.5 Winglet departure

Without the stiffness of the wing extension upper skin, the winglet could continue to rotate outward, departing the airplane downward and aft. In the process, this would start to peel the wing extension lower skin from the forward spar, applying tensile loads to the forward spar lower surface rivets until failure. This is consistent with the state of the wing extension forward spar lower rivets as found during the investigation.

3.5.6 Aileron trailing edge damage

If the lower skin departed the airplane aft, the skin debris could contact the aileron trailing edge almost directly behind the inboard edge of the wing extension as it departed the airplane, scratching and denting

the aileron trailing edge. See below for a view of the aileron trailing edge as found on the accident airplane.

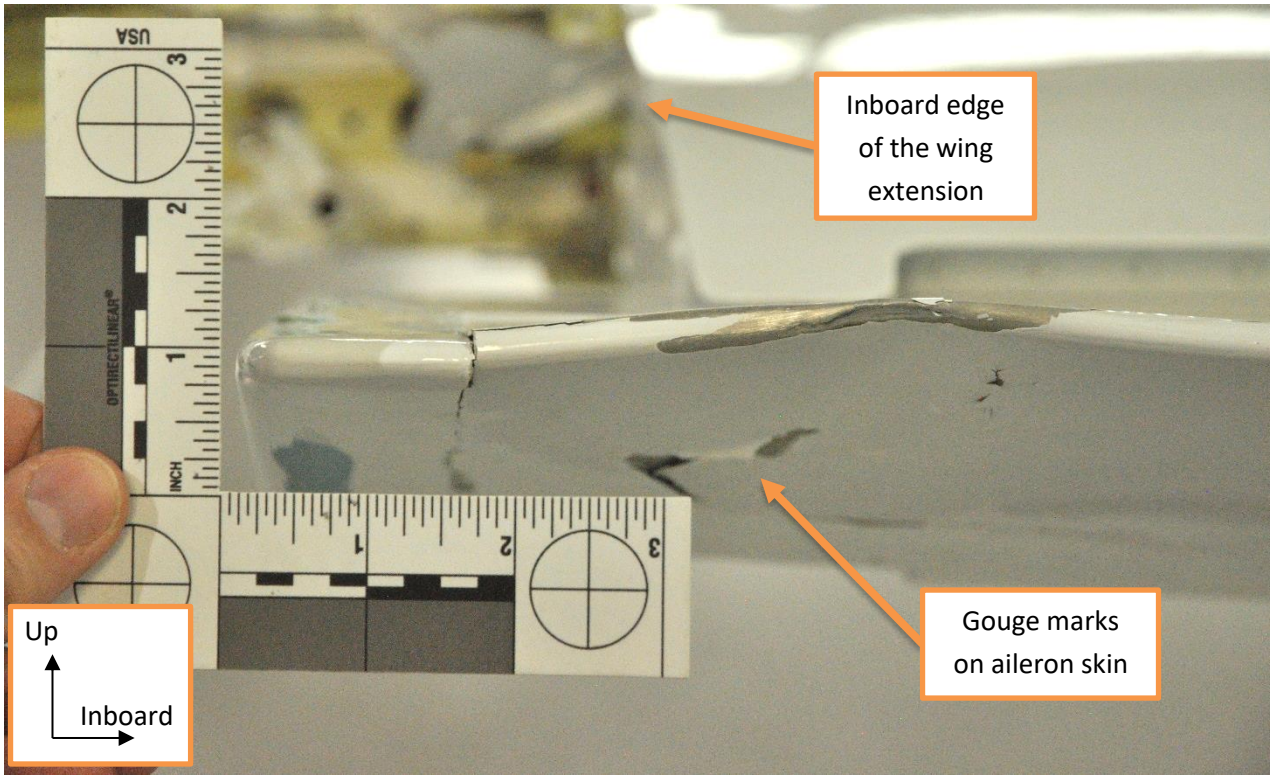

Figure 3-16 Aileron trailing edge damage as found (view looking forward)

The departing lower skin could also leave the small fiber of the aviation sealant on the aileron static wick as found in the process. The wing extension uses a similar type of sealant throughout the assembly, notably around the edges of the wing extension skin as a gap-filler. The sealant fiber was accompanied by material transfer oriented aft on the lower aileron skin and additional physical damage to the trailing edge. The material was collected and tested, but no conclusive determination could be made regarding its

composition. It is possible that the material was polysulfide sealant of the same type that was deposited on the aileron static wick. See below for illustration.

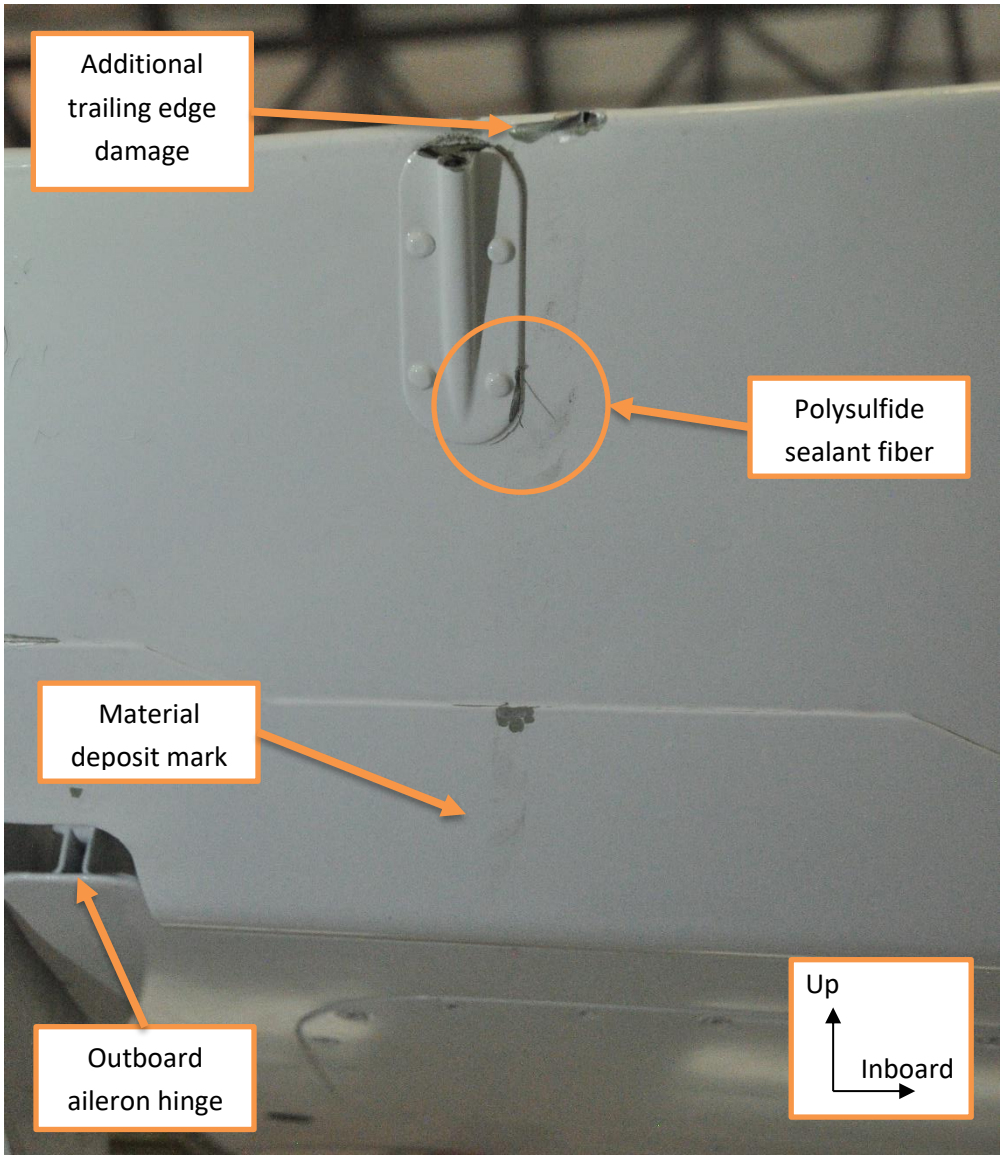

Figure 3-17 Aileron static wick fiber and aileron skin marks (view looking forward, aileron deflected up)

3.5.7 TACS departure from the airplane

The winglet departing the airplane would still be connected to the TACS via the outboard TACS hinge. The TACS hinge was found attached to the winglet, with evidence that the TACS hinge bearing tore out of the TACS hinge. The most likely explanation for this failure is overload as the winglet rotated down and outboard.

The aileron tip cap was also discovered with evidence of hard contact oriented inboard, most likely from the TACS rotating about the inboard hinge as the winglet separated from the wing extension and pulled the outboard TACS hinge aft.

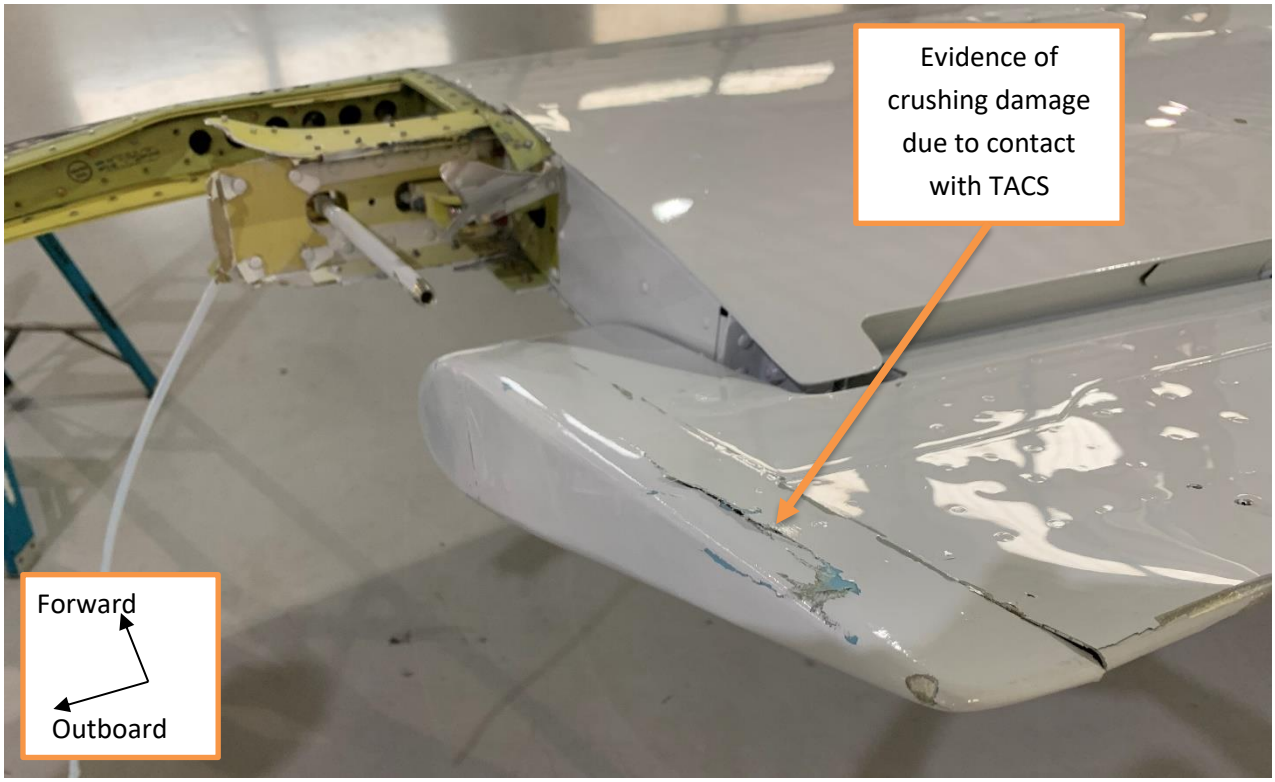

Figure 3-18 Aileron tip cap crushing damage (view looking forward and inboard)

3.5.8 Wing extension main spar departure

After the departure of the upper and lower skins of the wing extension and the winglet, the only structure available to support the TACS was the main spar, which was not designed to carry the extremely abnormal load exerted on it by the half-unsupported TACS and high dynamic pressure against the main spar web. The airplane was found with the TACS inboard hinge bracket completely separated from the remnants of

the main spar still attached to the airplane. See below for a view from the initial inspection of the accident airplane illustrating this.

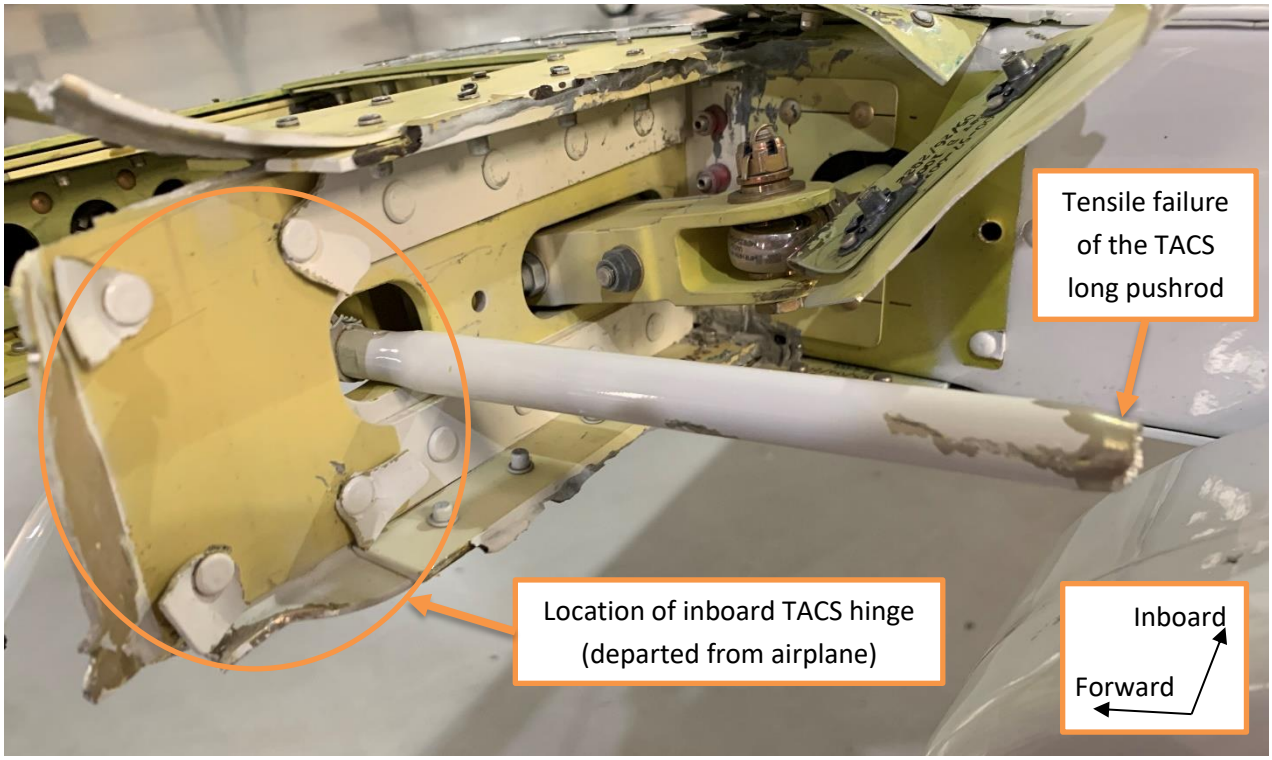

Figure 3-19 Inboard wing extension main spar and TACS kinematics remnants

This sequence of failures and departures of structure most likely occurred over a very short timeframe. The separation of the winglet and the TACS would likely have involved sudden changes in aerodynamic load on the structure just prior to failure and departure, which would most likely have been detectable in the cockpit. It is possible that the two sudden, short jolts reported by the pilot were related to the departure of the wing extension and winglet structures.

At the conclusion of this sequence of events, the TACS long pushrod remained protruding from the remnants of the wing extension main spar and bellcrank bracket. Severe gouging on the aileron balance horn lower surface indicates that the TACS pushrod was rubbing on the aileron, which would have been detectable in the flight controls. This is consistent with a pilot report of slight binding in the ailerons

during flight and landing, which could not be replicated during inspection of the accident aircraft after moving the long pushrod out of position. See below for an image of this damage.

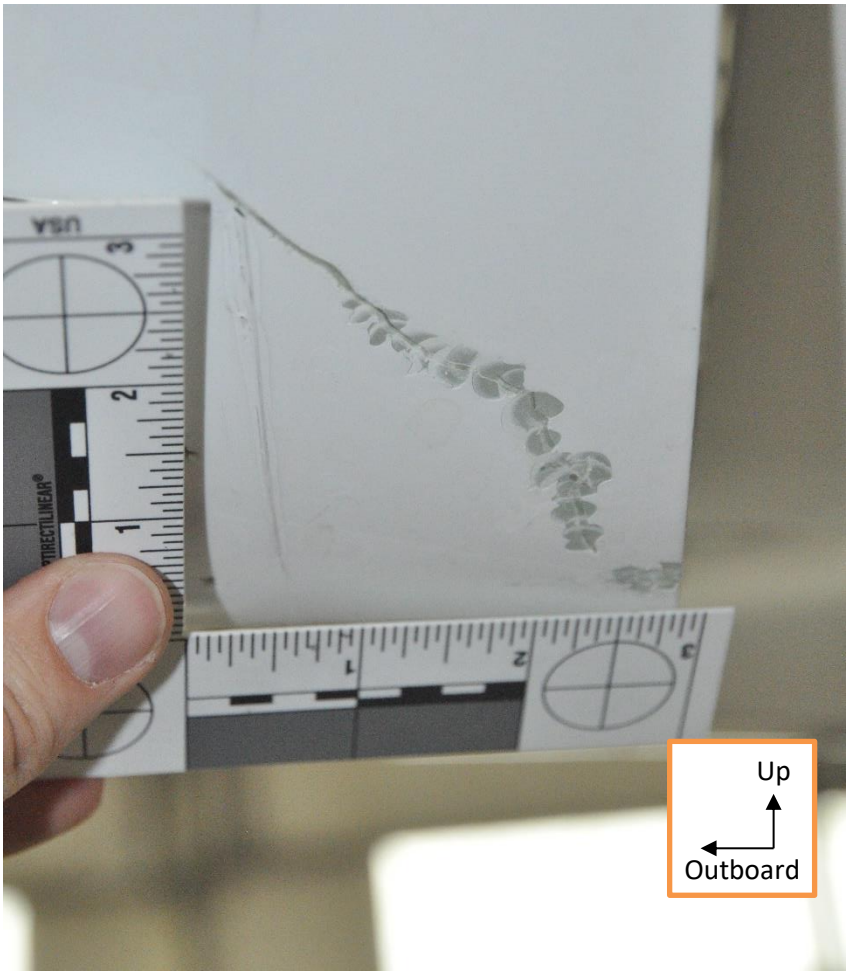

Figure 3-20 Aileron control horn gouging (view looking forward)

4 CONCLUSIONS

4.1 Tamarack Conclusion of Probable Cause

After extensive investigation, Tamarack concludes that the probable cause of this accident was in-flight overloading of the wing extension structure, caused by a reduction in structural capability due to undetected damage caused by a collision with an unknown object during ground operations.

4.2 Tamarack Safety Recommendations

As a result of this investigation, Tamarack recommends the following procedural clarifications for owners.

1. An increased emphasis on ground handling and taxiing best practices to avoid collisions with other objects, including allowance for additional space while maneuvering the lengthened wings around other aircraft and vehicles, ground observers on wingtips during towing operations, and additional care when operating doors or moving heavy equipment around the airplane.
2. Special attention given to preflight inspection of the winglet structure, noting particularly that the winglet tip cap is not readily visible to ground observers close to the airplane. Tamarack recommends moving back from the airplane to allow a better viewing angle, or using a stepladder or stepstool to raise the observer's eyeline closer to the winglet tip.
3. Additional scrutiny of the wing extension structure during preflight inspection, looking for the sudden appearance of cracked or blistered paint, exposed fasteners, or enlarged gaps, in accordance with good preflight inspection techniques generally applicable to all aircraft of this type.

APPENDIX A. LOAD CASES CONSIDERED DURING CERTIFICATION

Maneuver	CS-23 Section	SubCase	Mass Cases	Altitudes (ft)	Speeds	Total/ Incremental	Demand	Balance	Constrained Variables	Constrained Freedoms[1]	Flaps (deg)
Steady Pitching	23.333 (b) 23.337	3.6g	All	0, 8000, 20000, 26152 (Vd only), 29285, 40000², 45000 (not Va)	Va, Vd	Total	Nz, $\dot{\theta}$, TACS for g	Elev, α	$\ddot{\theta}$=0	1,2,4,6	Clean
		0g	All	0, 8000, 20000, 26152, 40000, 45000	Vd	Total	Nz, $\dot{\theta}$, TACS for g	Elev, α	$\ddot{\theta}$=0	1,2,4,6	Clean
		-1g	All	0, 8000, 20000, 29285, 40000, 45000	Vs, Vcd*	Total	Nz, $\dot{\theta}$, TACS for g	Elev, α	$\ddot{\theta}$=0	1,2,4,6	Clean
		-1.44g	All	0, 8000, 20000, 29285, 40000, 45000	Vs, Vc	Total	Nz, $\dot{\theta}$, TACS for g	Elev, α	$\ddot{\theta}$=0	1,2,4,6	Clean
Steady Pitching, Flaps	23.345	2g	All	0, 8000, 20000	Vf, Vsf, Vpf, Vspf	Total	Nz, $\dot{\theta}$, TACS for g	Elev, α	$\ddot{\theta}$=0	1,2,4,6	15, 35
		0g	All	0, 8000, 20000	Vf, Vsf, Vpf, Vspf	Total	Nz, $\dot{\theta}$, TACS for g	Elev, α	$\ddot{\theta}$=0	1,2,4,6	15, 35
Steady Pitching, Unsymmetrical Lift	23.349 (a) (2)	3.6g	All	0, 8000, 20000, 29285, 40000²	Va	Total	See section 3.3.9				Clean
Abrupt Pitching	23.423 (a)	Unchecked pull back	All	0, 8000, 20000, 29285, 40000²	Va	Incremental	Elev	$\ddot{\theta}$, α	$\dot{\theta}$=0, Nz = 0	1,2,4,6	Clean
	23.423 (a)	Unchecked push over	All	0, 8000, 20000, 29285, 40000²	Va	Incremental	Elev	$\ddot{\theta}$, α	$\dot{\theta}$=0, Nz = 0	1,2,4,6	Clean
	23.423 (b)	Checked 1g	All	0, 8000, 20000, 26152 (Vd only), 29285, 40000², 45000 (not Va)	Va, Vc, Vd	Incremental	$\ddot{\theta}$	Elev, α	$\dot{\theta}$=0, Nz = 0	1,2,4,6	Clean
	23.423 (b)	Checked 3.6g	All	0, 8000, 20000, 26152 (Vd only), 29285, 40000², 45000 (not Va)	Va, Vc, Vd	Incremental, added to 3.6g	$\ddot{\theta}$	Elev, α	$\dot{\theta}$=0, Nz = 0	1,2,4,6	Clean

Maneuver	CS-23 Section	SubCase	Mass Cases	Altitudes (ft)	Speeds	Total/ Incremental	Demand	Balance	Constrained Variables	Constrained Freedoms[1]	Flaps (deg)
Aircraft Gust Vertical (Tail-off)	23.341	Up	All	For Vb: 0, 8000, 20000, 30000, 37371, 45000 For Vc: 0, 8000, 20000, 29285, 40000, 45000 For Vd: 0, 8000, 20000, 26152, 40000, 45000	Vb, Vc, Vd	Incremental	Nz, TACS for g	$\ddot{\theta}$, α	$\dot{\theta}$=0	1,2,4,6	Clean
		Down	All	For Vb: 0, 8000, 20000, 30000, 37371, 45000 For Vc: 0, 8000, 20000, 29285, 40000, 45000 For Vd: 0, 8000, 20000, 26152, 40000, 45000	Vb, Vc, Vd	Incremental	Nz, TACS for g	$\ddot{\theta}$, α	$\dot{\theta}$=0	1,2,4,6	Clean
Aircraft Gust, Flaps	23.345	Up	All	0, 8000, 20000	Vf, Vpf	Incremental	Nz, TACS for g	$\ddot{\theta}$, α	$\dot{\theta}$=0	1,2,4,6	15, 35
		Down	All	0, 8000, 20000	Vf, Vpf	Incremental	Nz, TACS for g	$\ddot{\theta}$, α	$\dot{\theta}$=0	1,2,4,6	15, 35
Horizontal Tail Gust	23.425	N/A	All	0, 8000, 20000, 26152 (Vd only), 29285 (Vc only), 40000, 45000	Vc, Vd	Incremental	Unit α[3]	$\ddot{\theta}$, Nz	$\dot{\theta}$=0	1,2,4,6	Clean
Lateral Gust	23.443		All	For Vb: 0, 8000, 20000, 30000, 37371, 45000 For Vc: 0, 8000, 20000, 29285, 40000, 45000 For Vd: 0, 8000, 20000, 26152, 40000, 45000	Vb, Vc, Vd	Incremental	Unit β[3]	$\dot{r}$	r=0	1,2,3,4,5	Clean
Roll Maneuvers	23.455 (a) (2) (i)	Aileron Hardover	All	0, 8000, 20000, 29285, 40000[2]	Va	Incremental	Aileron	$\dot{p}$	p=0	1,2,3,5,6	Clean
	23.455 (a) (2) (ii)	Vc Roll Rate Match	All	0, 8000, 20000, 29285, 40000, 45000	Vc	Incremental	Aileron[4]	$\dot{p}$	p=0	1,2,3,5,6	Clean
	23.455 (a) (2) (iii)	Vd 1/3 Roll Rate Match	All	0, 8000, 20000, 26152, 40000, 45000	Vd	Incremental	Aileron[5]	$\dot{p}$	p=0	1,2,3,5,6	Clean
	23.349 (b)	Aileron Hardover – 2.4g[6]	All	0, 8000, 20000, 29285, 40000[2]	Va	Incremental, added to 2.4g	Same Va increment as above.				Clean
	23.349 (b)	Vc Roll Rate Match – 2.4g[6]	All	0, 8000, 20000, 29285, 40000, 45000	Vc	Incremental, added to 2.4g	Same Vc increment as above.				Clean
	23.349 (b)	Vd 1/3 Roll Rate Match – 2.4g[6]	All	0, 8000, 20000, 26152, 40000, 45000	Vd	Incremental, added to 2.4g	Same Vd increment as above.				Clean

Maneuver	CS-23 Section	SubCase	Mass Cases	Altitudes (ft)	Speeds	Total/ Incremental	Demand	Balance	Constrained Variables	Constrained Freedoms[1]	Flaps (deg)
		Aileron Hardover, Flaps	All	0, 8000, 20000	Vf, Vpf	Incremental	Aileron	$\dot{p}$	p=0	1,2,3,5,6	15, 35
Yaw Maneuvers	23.441 (b) (1)	Dynamic Overshoot	All	0, 8000	Vd	Incremental	β, $\dot{r}$	Rudder		1,2,3,4,5	Clean
	23.441 (b) (2)	Rudder Return Neutral at Max Steady Sideslip	All	0, 8000	Vd	Incremental	β, $\dot{r}$	Rudder		1,2,3,4,5	Clean
Failure Cases CoF		TACS Non-operative	All	0	Vk	Incremental	Nz	Elev, α	$\ddot{\theta}$=0	1,2,4,6	Clean
		TACS Hardover Symmetrical Up	All	0	Vk	Incremental	Nz	Elev, α	$\ddot{\theta}$=0	1,2,4,6	Clean
		TACS Hardover Symmetrical Down	All	0	Vk	Incremental	Nz	Elev, α	$\ddot{\theta}$=0	1,2,4,6	Clean
		TACS Hardover up, right only	All	0	Vk	Incremental	Nz	Elev, α, ailerons	$\ddot{\theta}$=0	1,2,6	Clean
		TACS Hardover down, right only	All	0	Vk	Incremental	Nz	Elev, α, ailerons	$\ddot{\theta}$=0	1,2,6	Clean
		TACS Hardover asymmetric, right up, left down	All	0	Vk	Incremental	Nz	Elev, α, ailerons	$\ddot{\theta}$=0	1,2,6	Clean
		TACS Hardover up, left only	All	0	Vk	Incremental	Nz	Elev, α, ailerons	$\ddot{\theta}$=0	1,2,6	Clean
		TACS Hardover down, left only	All	0	Vk	Incremental	Nz	Elev, α, ailerons	$\ddot{\theta}$=0	1,2,6	Clean
		TACS Hardover asymmetric, left up, right down	All	0	Vk	Incremental	Nz	Elev, α, ailerons	$\ddot{\theta}$=0	1,2,6	Clean
Failure Cases ToO		TACS Non-operative	All	29285	Vc	Total	Nz	Elev, α	$\ddot{\theta}$=0	1,2,4,6	Clean
		TACS Hardover Symmetrical Up	All	29285	Vc	Total	Nz	Elev, α	$\ddot{\theta}$=0	1,2,4,6	Clean
		TACS Hardover Symmetrical Down	All	29285	Vc	Total	Nz	Elev, α	$\ddot{\theta}$=0	1,2,4,6	Clean
		TACS Hardover up, right only	All	29285	Vc	Total	Nz	Elev, α, ailerons	$\ddot{\theta}$=0	1,2,6	Clean
		TACS Hardover down, right only	All	29285	Vc	Total	Nz	Elev, α, ailerons	$\ddot{\theta}$=0	1,2,6	Clean

Maneuver	CS-23 Section	SubCase	Mass Cases	Altitudes (ft)	Speeds	Total/ Incremental	Demand	Balance	Constrained Variables	Constrained Freedoms[1]	Flaps (deg)
		TACS Hardover asymmetric, right up, left down	All	29285	Vc	Total	Nz	Elev, α, ailerons	$\ddot{\theta}$=0	1,2,6	Clean
		TACS Hardover up, left only	All	29285	Vc	Total	Nz	Elev, α, ailerons	$\ddot{\theta}$=0	1,2,6	Clean
		TACS Hardover down, left only	All	29285	Vc	Total	Nz	Elev, α, ailerons	$\ddot{\theta}$=0	1,2,6	Clean
		TACS Hardover asymmetric, left up, right down	All	29285	Vc	Total	Nz	Elev, α, ailerons	$\ddot{\theta}$=0	1,2,6	Clean

[1] Freedoms numbered 1-6 following global axis system convention, x, y, z, rx, ry, rz.

[2] Nominal 40,000ft for Va cases is actually the max altitude limit where Va = Mc, which depends on aircraft mass (varying between 33,656ft and 43,464ft).

[3] A unit deflection is solved and factored in the post process to match appropriate requirement.

[4] Max aileron scaled by Va/Vc ratio.

[5] Max aileron scaled by Va/3Vd ratio. Accounting for difference in altitude between some Va and Vd cases.

[6] 2.4g steady load for roll maneuvers generated using same method as Steady Pitching 3.6g case, including appropriate levels of TACS.

* Vcd = linearly interpolated speed between Vc and Vd for -1g steady maneuver cases, where 0g loads are calculated at Vd and -1.44g loads are calculated at Vc.

APPENDIX B. DETAILS OF CRITICAL LOADS CASES FOR THE WINGLET AND WING EXTENSION

	Critical Shear Cases						
Wing Extension	FS [in]	BL [in]	WL [in]	Max [lbf]	Max Case	Min [lbf]	Min Case
	304.28	311.03	111.16	884	3X08GUA1599	-919	2_ACGUA0234
	304.36	316.4	111.63	663	3X08GUA1599	-693	2_ACGUA0234
	304.51	327.2	112.57	427	3X08GUA1599	-379	2_ACGUA0234
	304.62	335.4	113.29	230	3X08GUA1599	-243	2XYA56B0232
	304.77	346.15	114.23	211	2XYA56A1332	-243	2XYA56B0232
Winglet	FS [in]	BL [in]	WL [in]	Max [lbf]	Max Case	Min [lbf]	Min Case
	304.77	346.15	114.23	470	2XYA56A1332	-437	2XYA56B0232
	309.87	348.27	121.92	349	2XYA56A1332	-332	2XYA56B0232
	314.98	350.36	129.61	243	2XYA56A1332	-230	2XYA56B0232
	320.07	352.44	137.27	155	2_YA56A1332	-147	2_YA56B0232
	325.15	354.52	144.93	38	2_YA56A1332	-36	2_YA56B0232
	333.24	357.83	157.12	38	2_YA56A1332	-36	2_YA56B0232

Case	Aircraft Configuration	Speedbrake Status	Failure Condition	Case Description	Attitude	Mass Case	Speed	Altitude
3X08GUA1599	Continuation of Flight Failure	Extended	TACS Hardover Symmetrical Down, Elevator Balance	Aircraft Gust Up	Straight and Level	MTOW, Fwd CG	Vk 160 KCAS	0
2XYA56A1332	ATLAS Operative	Extended	N/A	Yaw Maneuver - Commuter Dynamic Overshoot	Nose Slip Left	MTOW High Iyy, Izz	Vd 325 KCAS	8000
2_YA56A1332	ATLAS Operative	Rectracted	N/A	Yaw Maneuver - Commuter Dynamic Overshoot	Nose Slip Left	MTOW High Iyy, Izz	Vd 325 KCAS	8000
2_ACGUA0234	ATLAS Operative	Rectracted	N/A	Aircraft Gust Up	Straight and Level	Min Weight, Aft CG	Vd 325 KCAS	26,152
2XYA56B0232	ATLAS Operative	Extended	N/A	Yaw Maneuver - Commuter Dynamic Overshoot	Nose Slip Right	Min Weight, Aft CG	Vd 325 KCAS	8000
2_YA56B0232	ATLAS Operative	Rectracted	N/A	Yaw Maneuver - Commuter Dynamic Overshoot	Nose Slip Right	Min Weight, Aft CG	Vd 325 KCAS	8000

	Critical Bending Moment Cases						
Wing Extension	FS [in]	BL [in]	WL [in]	Max [in-lbf]	Max Case	Min [in-lbf]	Min Case
	304.28	311.03	111.16	23985	3X08GUA1599	-23190	2XYA56B0232
	304.36	316.4	111.63	19013	3X08GUA1599	-20128	2XYA56B0232
	304.51	327.2	112.57	14730	2XYA56A1332	-15211	2XYA56B0232
	304.62	335.4	113.29	12569	2XYA56A1332	-12249	2XYA56B0232
	304.77	346.15	114.23	10293	2_YA56A1332	-9624	2_YA56B0232
Winglet	FS [in]	BL [in]	WL [in]	Max [in-lbf]	Max Case	Min [in-lbf]	Min Case
	304.77	346.15	114.23	10058	2_YA56A1332	-9436	2_YA56B0232
	309.87	348.27	121.92	6381	2_YA56A1332	-6020	2_YA56B0232
	314.98	350.36	129.61	3626	2_YA56A1332	-3435	2_YA56B0232
	320.07	352.44	137.27	1719	2_YA56A1332	-1631	2_YA56B0232
	325.15	354.52	144.93	473	2_YA56A1332	-446	2_YA56B0232
	333.24	357.83	157.12	5	2_YA56B0232	-5	2_YA56A1332

Case	Aircraft Configuration	Speedbrake Status	Failure Condition	Case Description	Attitude	Mass Case	Speed	Altitude
3X08GUA1599	Continuation of Flight Failure	Extended	TACS Hardover Symmetrical Down, Elevator Balance	Aircraft Gust Up	Straight and Level	MTOW, Fwd CG	Vk 160 KCAS	0
2XYA56A1332	ATLAS Operative	Extended	N/A	Yaw Maneuver - Commuter Dynamic Overshoot	Nose Slip Left	MTOW High Iyy, Izz	Vd 325 KCAS	8000
2_YA56A1332	ATLAS Operative	Rectracted	N/A	Yaw Maneuver - Commuter Dynamic Overshoot	Nose Slip Left	MTOW High Iyy, Izz	Vd 325 KCAS	8000
2XYA56B0232	ATLAS Operative	Extended	N/A	Yaw Maneuver - Commuter Dynamic Overshoot	Nose Slip Right	Min Weight, Aft CG	Vd 325 KCAS	8000
2_YA56B0232	ATLAS Operative	Rectracted	N/A	Yaw Maneuver - Commuter Dynamic Overshoot	Nose Slip Right	Min Weight, Aft CG	Vd 325 KCAS	8000

	Critical Torsion Cases						
Wing Extension	FS [in]	BL [in]	WL [in]	Max [in-lbf]	Max Case	Min [in-lbf]	Min Case
	304.28	311.03	111.16	2502	2XACGUA0234	-4655	2_YA56A1332
	304.36	316.4	111.63	2164	2XACGUA0234	-3958	2_YA56A1332
	304.51	327.2	112.57	1706	2_YA56B0232	-3144	2_YA56A1332
	304.62	335.4	113.29	2082	2_YA56B0232	-2493	2_YA56A1332
	304.77	346.15	114.23	2045	2_YA56B0232	-2462	2_YA56A1332
Winglet	FS [in]	BL [in]	WL [in]	Max [in-lbf]	Max Case	Min [in-lbf]	Min Case
	304.77	346.15	114.23	6405	2XYA56B0232	-6964	2XYA56A1332
	309.87	348.27	121.92	4039	2XYA56B0232	-4278	2XYA56A1332
	314.98	350.36	129.61	2245	2XYA56B0232	-2368	2XYA56A1332
	320.07	352.44	137.27	1087	2_YA56B0232	-1143	2_YA56A1332
	325.15	354.52	144.93	212	2_YA56B0232	-223	2_YA56A1332
	333.24	357.83	157.12	84	2_YA56A1332	-77	2_YA56B0232

Case	Aircraft Configuration	Speedbrake Status	Failure Condition	Case Description	Attitude	Mass Case	Speed	Altitude
2XACGUA0234	ATLAS Operative	Extended	N/A	Aircraft Gust Up	Straight and Level	Min Weight, Aft CG	Vd 325 KCAS	26,152
2_YA56B0232	ATLAS Operative	Retracted	N/A	Yaw Maneuver - Commuter Dynamic Overshoot	Nose Slip Left	Min Weight, Aft CG	Vd 325 KCAS	8,000
2XYA56B0232	ATLAS Operative	Extended	N/A	Yaw Maneuver - Commuter Dynamic Overshoot	Nose Slip Left	Min Weight, Aft CG	Vd 325 KCAS	8,000
2_YA56A1332	ATLAS Operative	Retracted	N/A	Yaw Maneuver - Commuter Dynamic Overshoot	Nose Slip Right	MTOW High Iyy, Izz	Vd 325 KCAS	8,000
2XYA56A1332	ATLAS Operative	Extended	N/A	Yaw Maneuver - Commuter Dynamic Overshoot	Nose Slip Right	MTOW High Iyy, Izz	Vd 325 KCAS	8,000